https://doi.org/10.5194/wcd-2021-61
Preprint. Discussion started: 1 October 2021


Weather and Climate Dynamics Discussions
Open Access
EGU

# Achieving realistic Arctic-midlatitude teleconnections in a climate model through stochastic process representation

Kristian Strommen[1] and Stephan Juricke[2,3]

[1]University of Oxford, Oxford, United Kingdom
[2]Mathematics and Logistics, Jacobs University, Bremen, Germany
[3]Alfred Wegener Institute, Helmholtz Centre for Polar and Marine Research, Bremerhaven, Germany

**Correspondence:** Kristian Strommen (kristian.strommen@physics.ox.ac.uk)

**Abstract.** The extent to which interannual variability in Arctic sea ice influences the midlatitude circulation has been extensively debated. While observational data supports the existence of a teleconnection between November sea ice in the Barents-Kara region and the subsequent winter circulation, climate models do not consistently reproduce such a link, with only very weak inter-model consensus. We show, using the EC-Earth3 climate model, that while a deterministic ensemble of coupled simulations shows no evidence of such a teleconnection, the inclusion of stochastic parameterizations to the ocean and sea ice component of EC-Earth3 results in the emergence of a robust teleconnection comparable in magnitude to that observed. We show that this can be accounted for entirely by an improved ice-ocean-atmosphere coupling due to the stochastic perturbations. In particular, the inconsistent signal in existing climate model studies may be due to model biases in surface coupling, with stochastic parameterizations being one possible remedy.

## 1 Introduction

Over the last several decades, Arctic sea ice has been undergoing a precipitous decline (Stroeve and Notz (2018)). Since this loss is unanimously projected to continue as long as greenhouse gas concentrations keep increasing (Notz and Community (2020)), a considerable number of studies have been devoted to understanding what influence this may or may not have on mid-latitude weather and climate (see, e.g., Barnes and Screen (2015) for a good overview). The role of sea ice variability in driving mid-latitude weather has also been extensively examined on interannual timescales, where it has, in particular, been suggested as a key source of predictability in seasonal forecasts of Euro-Atlantic boreal winter (García-Serrano et al. (2015); Dunstone et al. (2016); Kretschmer et al. (2016); Wang et al. (2017)). Of central importance on both climate and seasonal timescales is a proposed teleconnection between November sea ice concentration in the Barents-Kara (BK) region and the December-January-February (DJF) North Atlantic Oscillation (NAO), where a negative sea ice anomaly forces a negative NAO anomaly (Deser et al. (2007); Sun et al. (2015)). Because the NAO is the dominant mode of variability in the Euro-Atlantic sector (Hurrell et al. (2003)), such a teleconnection would provide a direct pathway for sea ice variability to affect the mid-latitudes.

Both tropospheric and stratospheric mechanisms have been suggested for such a teleconnection. In the tropospheric pathway, localized heat flux anomalies triggered by the exposure of the relatively warm ocean to the cold Arctic atmosphere may trigger

https://doi.org/10.5194/wcd-2021-61
Preprint. Discussion started: 1 October 2021


Weather and Climate Dynamics Discussions
Open Access
EGU

stationary Rossby wave anomalies Hoskins and Karoly (1981) which can subsequently grow to a large-scale NAO response García-Serrano et al. (2015). The stratospheric pathway posits that these waves may penetrate all the way up to the stratosphere, where they break and weaken the polar vortex: this would be expected to result in an NAO response at the surface in late winter Peings and Magnusdottir (2014); Kim et al. (2014). The importance of a favorable North Atlantic storm track has been emphasized for both mechanisms Deser et al. (2007); Strong and Magnusdottir (2010); Siew et al. (2020).

However, there is currently no consensus in the literature on whether this teleconnection actually exists at all. While studies looking for predictors of the winter NAO in reanalysis data frequently identify a robust BK-NAO teleconnection as the largest source of predictability (Kretschmer et al. (2016); Wang et al. (2017)), this is not straightforwardly reproduced using climate model experiments. Indeed, while models do, on the whole, show a consistent NAO response to imposed sea ice anomalies, the signal appears to be both much smaller and less consistent, with considerable variability across models (see, e.g., Screen et al. (2018) for an overview). More seriously, long climate simulations of a single model with fixed forcing exhibit decade-long periods where the correlation between BK sea ice and the NAO can be both positive, negative or zero (Koenigk and Brodeau (2017)), leading some to suggest that the apparently significant positive correlation seen in the recent observational record is purely a result of atmospheric internal variability (ibid; Warner et al. (2020); Blackport and Screen (2021)). Notably, Blackport et al. (2019) argued that the teleconnection signals seen in both reanalysis and two climate models could be entirely accounted for by atmospheric forcing, though it should be noted that the analysis was essentially indirect, with no concrete common driver of both November sea ice and the winter NAO being proposed. The later study by Warner et al. (2020) explicitly suggested tropical forcing might be one such common driver.

The situation is further complicated by the discovery in recent years of a so-called signal-to-noise paradox in seasonal forecasts of the winter NAO (Scaife and Smith (2018)). This paradox, in essence, is the fact that while forecast models initialised in November can now produce DJF NAO predictions that correlate remarkably well with the observed NAO, the signal is extremely weak in the forecast models and high correlations can only be realised by taking the mean across a large ensemble forecast (Eade et al. (2014); Dunstone et al. (2016)). In particular, the size of the signal compared to the level of skill (i.e., the magnitude of the correlation) implies that the real world may be significantly more predictable than the models think it is. One possible explanation for this is that models have systematically under-persistent circulation anomalies (Strommen and Palmer (2019)), but another is that models fail to capture real-world teleconnections adequately (Siegert et al. (2016)). This raises the possibility that the Arctic-NAO teleconnection is real, and that the weak and inconsistent signals seen in climate model simulations is a manifestation, or possibly even the cause, of the signal-to-noise paradox. While some studies, such as Blackport and Screen (2021), argue that the overall signal is too small to be robust even when using large ensembles of climate simulations, it has been noted in Baker et al. (2018) that not all seasonal forecast models exhibit skillful winter NAO forecasts. It is therefore not obvious, a priori, that all the climate models considered in studies such as Blackport and Screen (2021) represent the relevant processes correctly. This naturally begs the question: what processes might not be represented correctly in state-of-the-art climate models that could inhibit a realistic Arctic-NAO teleconnection?

In this paper, we will study the impact of including the stochastic parameterization schemes of Juricke et al. (2013); Juricke and Jung (2014) to the sea ice component and of Juricke et al. (2017) to the ocean component of the fully coupled EC-Earth3

https://doi.org/10.5194/wcd-2021-61
Preprint. Discussion started: 1 October 2021


Weather and Climate Dynamics Discussions
Open Access
EGU

climate model. Stochastic schemes aim to represent the influence of uncertain processes, such as unresolved sub grid-scale physics, using carefully calibrated random noise. The potential for such schemes to radically improve weather forecasts is well known (Palmer et al. (2009); Sanchez et al. (2015); Berner et al. (2017)), and a growing body of literature now suggests that such schemes can also have a beneficial impact on climate model simulations as well (see, e.g., Dawson and Palmer (2015); Watson et al. (2017); Christensen et al. (2017); Juricke et al. (2017); Strommen et al. (2019); Vidale et al. (2021) for some examples). Of particular relevance is the suggestion of Strømmen et al. (2017) that stochasticity can in some cases make teleconnections more realistic. We compare an ensemble of three deterministic simulations (labelled CTRL) spanning 1950-2015, with an equivalent ensemble (labelled OCE) with stochastic sea ice and ocean parameterizations active. The model used is a fully coupled version of EC-Earth3: see Data and Methods for details of the stochastic schemes and the model. We will show that while the CTRL simulations do not exhibit a systematic relationship between sea ice and the NAO, the OCE simulations appear to systematically recover a significant teleconnection comparable to that seen in the reanalysis product ERA5. Analysis using a linear inverse model (LIM), along with comparisons against simulations with forced sea-surface temperatures (SSTs) and sea ice, strongly suggests that the stochastic schemes are primarily acting to improve the coupling between the atmosphere, ocean, and sea ice on daily timescales. The ability of stochastic schemes to profoundly impact atmosphere-ocean coupling has already been observed in, e.g., Christensen et al. (2017). Our results therefore imply that inadequate ice-ocean-atmosphere coupling may be a key bias contributing to the weak and inconsistent ice-NAO teleconnection in climate models and that stochastic schemes may alleviate such biases.

The structure of the paper is as follows. In Section 2 we describe the model and simulation setup, the stochastic ocean and sea ice schemes and the diagnostic methods used in this study. Section 3 discusses the effects of the stochastic schemes on the climatology of the model, while Section 4 focuses specifically on the impact of the schemes on the Arctic-NAO teleconnections in EC-Earth3 and compares the modelled teleconnections to observational estimates. In Section 5 we provide some explanations for improved teleconnections with the stochastic sea ice and ocean schemes due to improved ice-ocean-atmosphere coupling and Section 6 discusses some alternative explanations not directly related to improved (high latitude) coupling. Finally, Section 7 consists of a discussion of the results and some final conclusions.

## 2 Data and Methods

### 2.1 The EC-Earth3 model and description of stochastic schemes

The model used for the coupled climate simulations in this study is a version of EC-Earth3. Specifically, we use the EC-Earth3P configuration developed for the HighResMIP protocol, as described in Haarsma et al. (2020). It is very closely related to the version that was used for the introduction of the probabilistic Earth system model in Strommen et al. (2019). In their study, the focus was on stochasticity in the atmospheric and land surface component of uncoupled atmosphere-only simulations, while in this study the stochasticity is placed in the ocean and sea ice model component as discussed below.

The atmospheric model component of EC-Earth consists of a modified version of the Integrated Forecast System (IFS) developed and used at the European Centre for Medium Range Weather Forecasts (ECMWF). It includes the the land surface model

https://doi.org/10.5194/wcd-2021-61
Preprint. Discussion started: 1 October 2021


Weather and Climate Dynamics Discussions
Open Access
EGU

Hydrology Tiled ECMWF Scheme of Surface Exchanges over Land (H-TESSEL) (Balsamo et al. (2009)). The ocean model component is represented by the NEMO model version 3.6 (Madec and the NEMO team (2016)) which includes the LIM3 sea ice model (Vancoppenolle et al. (2012)). The atmospheric model is run at a spectral resolution of T255, which corresponds to an approximate grid spacing of 80km at the equator, with 91 vertical layers. Note that this model produces a reasonable looking quasi-biennial oscillation (Strommen and Palmer (2019)). NEMO is run at a resolution of around 1° with 75 vertical layers. Note that, as discussed in Haarsma et al. (2020), the original NEMO configuration for EC-Earth3P produced an Atlantic Meridional Overturning Circulation (AMOC) with unrealistically low values: the configuration used in these experiments corresponds to the $p2$ configuration discussed in ibid, and therefore does have a realistic AMOC. We also note that the EC-Earth3P model was tuned to represent a realistic top of the atmosphere energy budget compared to observational estimates for the time period 1990-2010.

The two types of coupled simulations carried out in this study differ only by the use of stochastic parametrizations in the ocean and sea ice model component. The control simulation CTRL runs without any stochastic parametrizations turned on. The stochastic simulation OCE on the other hand has three stochastic ocean schemes (Juricke et al. (2017, 2018)) and one stochastic sea ice scheme (Juricke et al. (2013); Juricke and Jung (2014); Juricke et al. (2014)) switched on.

The stochastic ocean schemes are based on perturbations to

1. the classical Gent–McWilliams parametrization for eddy induced advection (Gent and Mcwilliams (1990)) used in coarse resolution, non eddy-resolving ocean simulations (henceforth StoGM);
2. the enhanced vertical diffusion parametrization which is used for unstable stratification (henceforth StoDV);
3. the turbulent kinetic energy (TKE) parametrization through which the amplitude of vertical diffusivity and viscosity are obtained (henceforth StoTKE);

For the deterministic control simulation, all above mentioned parametrization schemes are used in their default, non-stochastic form.

The stochastic ocean schemes have been explained in detail and tested in long ocean-only simulations by Juricke et al. (2017) and have also been tested in coupled seasonal forecasts by Juricke et al. (2018). These studies showed that the StoGM and StoTKE schemes in particular can have a considerable impact on near surface variability in regions of strong horizontal gradients (StoGM) or strong atmosphere-ocean interactions (StoTKE). The StoGM scheme showed the strongest impact on variability in western boundary currents such as the Kuroshio and the Southern Ocean, as it varies the effective amplitude of eddy induced temperature and salinity advection. The StoTKE scheme on the other hand had a pronounced impact on variability and mean state in the tropics and also in mid-latitudes, as it can affect the response of the mixed layer to atmospheric forcing. The StoDV scheme showed only a very limited response in these previous studies, as its variations only matter in areas of deep convection in the high latitudes and even there only at times of strong and deep convective activity. However, the effect of these schemes has so far not been tested in long (multidecadal) coupled simulations.

https://doi.org/10.5194/wcd-2021-61
Preprint. Discussion started: 1 October 2021


Weather and Climate Dynamics Discussions
Open Access
EGU

For the sea ice, the stochastic scheme implemented is the stochastic sea ice strength parametrization (henceforth StoSIS) by Juricke et al. (2013), which has so far been tested in ocean-only simulations with the Alfred Wegener Institute (AWI) sea ice-ocean model FESOM (Juricke et al., 2013); with NEMO (Brankart et al., 2015); in annual coupled seasonal ensemble simulations (Juricke et al., 2014); and finally in coupled climate simulations (Juricke and Jung, 2014) with the AWI-CM climate model. The scheme perturbs the resistance of sea ice to convergent motion, which can lead to plastic deformation in the sea ice model. This corresponds to the ridging of sea ice. Ridging can create sea ice of thicknesses beyond the thermodynamic equilibrium thickness of around 1-3 m (depending on local conditions and hemispheric differences between the Arctic and Antarctic) which can already be achieved by purely thermodynamic freezing of sea water. Especially for older multiyear ice in the Arctic, dynamic processes driven by convergent/divergent motion due to atmospheric or oceanic currents are dominating contributors when it comes to sea ice thickness distributions (Juricke et al., 2013). The StoSIS scheme simulates the variations and uncertainties in the local ice strength and can lead to either faster or slower ice convergence, where the non-linearity in the process leads to a stronger response for weak ice compared to strong ice (Juricke et al., 2013). Consequentially, ice tends to move faster under stochastic ice strength perturbations until the effect is balanced by thicker sea ice that also acts to strengthen the resistance towards plastic deformation. Furthermore, ridging tends to be stronger with StoSIS, especially along coastlines if the ice is moved towards the coast (Juricke et al., 2013). However, due to the strongly coupled system consisting of sea ice, atmosphere and ocean in the high latitudes, the climatological response both with respect to mean changes in the sea ice as well as surface flux variability varies between uncoupled (large increase in sea ice volume) and coupled (balancing increase of thick ice vs decrease of thinner ice) simulations (Juricke and Jung, 2014). The sensitive response of StoSIS and, consequently, sea ice dynamics to the atmospheric coupling is one of the main foci of this study.

### 2.2 Model simulations and observational data

For each of the two configurations CTRL and OCE, described in the previous section, three ensemble members were generated according to the *hist-1950* experimental protocol (Haarsma et al. (2020)). Each member is therefore initialised on January 1st 1950, and run with observed anthropogenic forcing until January 1st 2015: these simulations thereby span 65 years. Different ensemble members are created by slightly perturbing the upper air temperatures at 5 randomly chosen grid points: the atmospheric variability of the members are found to be effectively uncorrelated after just a few months.

To estimate the impact of mean state biases, we will also consider simulations with prescribed SSTs and sea-ice. A set of three deterministic ensemble members were generated in the same way by initial condition perturbation: each member then simulates the period 1950-2015. This ensemble, and its experimental configuration, will be referred to as AMIP. Note that in accordance with the HighResMIP Protocol, the prescribed forcing uses daily data, as opposed to the more common monthly forcing. This in principle allows the simulations to simulate more sub-seasonal variability.

In order to further assess the statistical significance of the teleconnection, we make use of additional deterministic coupled simulations using the slightly earlier version EC-Earth3.1, as generated for the Climate SPHINX Project (Davini et al. (2017)). The data we make use of consists of three ensemble members spanning the period 1900-2015 using historical forcings.

https://doi.org/10.5194/wcd-2021-61
Preprint. Discussion started: 1 October 2021


Finally, for observational data, we make use of the ERA5 data set (Hersbach et al. (2020)). The OSI450 sea ice data set ((Lavergne et al., 2019)) is also used in Section 4.1 to compare the teleconnection region identified in ERA5.

### 2.3 Methods

The NAO is defined, for each data set, as the leading principal component (PC) of daily, detrended geopotential height anomalies at 500hPa (zg500). The sign of the principal component is imposed to make the corresponding empirical orthogonal function match the standard NAO pattern. Because we will be making use of daily data, a daily climatology is directly fitted to the data and subtracted from the daily PC. All available data is used for each data set, though no meaningful differences were found if this procedure was carried out using, e.g., only data from 1980 onwards.

Timeseries of daily sea-ice concentration (siconc) anomalies in a given region is computed by averaging over grid points, detrending and removing a directly fitted daily climatology. As with the NAO, this is done using all available data, before restricting to specific time periods. Two regions will be considered in this paper: Barents-Kara (BK), defined by the box 67N-80N, 30E-75E, and Barents-Greenland (BG), defined by the box 65N-82N, 5E-60E.

Correlations are computed as Pearson correlation coefficients. In plots showing correlations at multiple grid points, statistical significance at the 95% confidence interval is computed using the standard error. In plots showing changes to the mean state at grid points, significance is estimated with a two-tailed t-test, with no equal variance being assumed. In plots showing changes in the standard deviation at grid points, significance is estimated using the Bartlett test for SSTs, and the Levene test for sea ice. When computing correlations between sea ice and NAO timeseries (as in Table 11), a null hypothesis of each timeseries as an AR1 process is assumed. By fitting such a process to each timeseries and simulating 10,000 random draws, we obtain confidence intervals for the correlations expected by chance. For ERA5 and the individual ensemble members of CTRL and OCE, which have a sample size of 35 (covering the 35 complete DJF seasons between January 1980 and December 2015), a 95% confidence interval is approximately given by $\pm 0.35$. For the concatenated timeseries of CTRL and OCE, which have a larger sample size of $35 \cdot 3 = 105$, the 95% confidence interval is approximately $\pm 0.2$, with a 99% interval given by $\pm 0.24$.

Taking ensemble means does not make sense for free-running models, so instead, when evaluating differences in time series between the CTRL and OCE ensembles (of the NAO, sea ice, or some grid point), the time series of each ensemble member are typically concatenated back to back prior to comparison. Note that in a standard forecasting context, where one is comparing an ensemble of forecasts $x_i$ for $i = 1, \ldots, N$, against a fixed observational time series $y$, the correlation between the ensemble mean and $y$ equals the correlation between the time series of the concatenated members $x_i$ and the time series obtained by concatenating $y$ with itself $N$ times. Therefore, the concatenated time series can be thought of as a natural extension of the ensemble mean which makes sense even when the 'observed' time series $y$ is no longer fixed (as is the case when comparing CTRL and OCE).

Finally, in this paper we will generally focus on the 35 winters between 1980 and 2015, where observational estimates are particularly trustworthy. Teleconnections in model data will be considered over earlier time periods as a test of significance and consistency.

https://doi.org/10.5194/wcd-2021-61
Preprint. Discussion started: 1 October 2021


## 3 Impact on the climate mean state

We first show the impact of the stochastic schemes on the long-term mean and variability of the model, noting that the impact of the stochastic ocean schemes in longer coupled simulations with EC-Earth has not previously been documented in the literature.

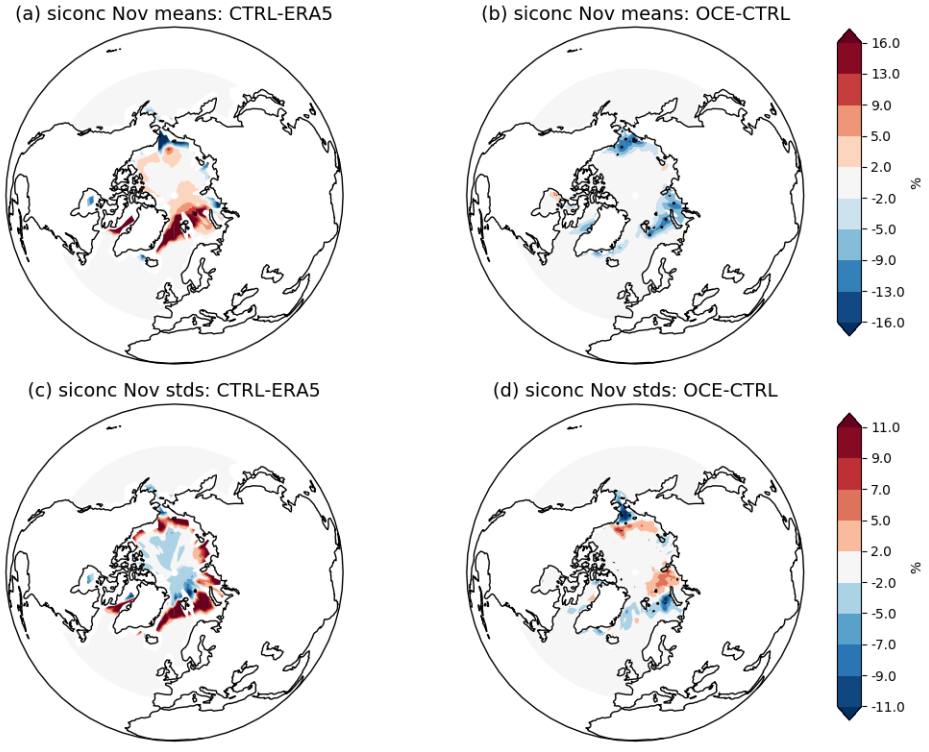


**Figure 1.** Sea ice concentration (mean and standard deviations) in November. Mean quantities in (a) CTRL-ERA5 and (b) OCE-CTRL. Standard deviations in (c) CTRL-ERA5 and (d) OCE-CTRL. Stippling in (b) and (d) highlights gridpoints where the change is statistically significant ($p<0.05$); in (a) and (c) almost every gridpoint outside the zero contour is significant so stippling is not included for visual ease. The period considered is 1980-2015.

Figure 1 shows the differences in the mean and standard deviation of sea ice concentration (siconc) for CTRL versus ERA5, as well as the impact on these differences in OCE, across 35 November months from the period 01-01-1980 to 31-12-2015; note that data is only drawn from the 35 winters spanning a full November-February season. A significant bias around the Greenland and Barents seas can be seen in the CTRL experiments, with the model producing too much sea ice with excessive interannual variability. The OCE model considerably reduces the mean state bias in the Barents sea, with only a limited impact on the Greenland sea bias. The bias in the standard deviation is also reduced, both in the Barents and Greenland seas, though the changes are not significant at every gridpoint. Similarly, the CTRL bias in the Labrador sea is also reduced with OCE, both with respect to the mean and the variability, but these changes do not show up as significant. On the other hand, OCE appears

https://doi.org/10.5194/wcd-2021-61
Preprint. Discussion started: 1 October 2021


to have a neutral or negative impact on the biases in the Kara and Bering seas. All these impacts were found to be qualitatively similar when considering the DJF period instead.

The general tendency for the StoSIS to reduced sea ice concentration along the ice edge due to stronger ice motion towards the coast of Greenland and the Canadian Arctic Archipelago has also been observed in coupled climate simulations with the AWI-CM model by (Juricke and Jung, 2014). This result is therefore consistent with their physical explanation of accelerated ice transport caused by an effective (non-linear) weakening of the sea ice by the random ice strength perturbations.

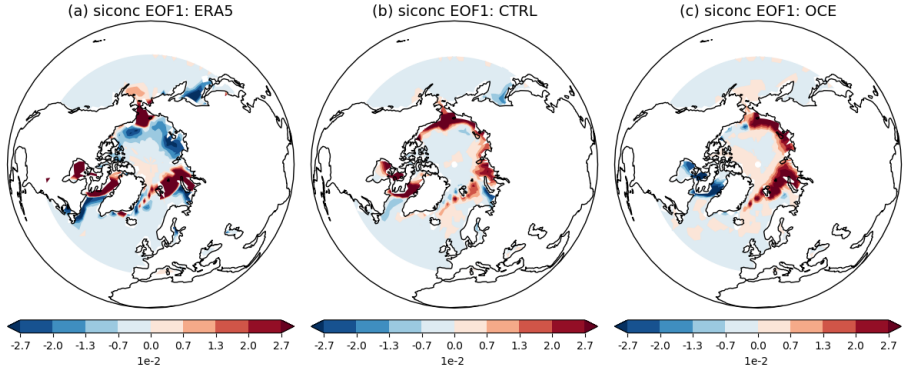


**Figure 2.** The first empirical orthogonal functions of November sea ice concentration in November for (a) ERA5, (b) CTRL and (c) OCE. The period considered is 1980-2015.

The changes in the mean and standard deviation in both model simulations with respect to ERA5 suggests that the general patterns of interannual sea ice variability are not the same in the reanalysis and the models. Figure 2 shows the leading empirical orthogonal function (EOF) of November sea ice for ERA5 and the model data, demonstrating that this is indeed the case, with all three data sets exhibiting visibly different EOFs. Of particular relevance to the topic of this paper is the fact that while both ERA5 and OCE show a lot of variability in the Barents-Kara region, the CTRL model has most of its variability concentrated in the Bering sea. This will be discussed further in the next section.

Figures 3 shows analogous differences in the mean and standard deviation of ssea surface temperatures (SSTs) for CTRL versus ERA5 and OCE. The only places where OCE appears to notably alter the mean state are the North Atlantic, Barents-Kara and Kuroshio region. The reduced bias in the Kuroshio region is consistent with the results of Juricke et al. (2017), which showed, using shorter simulations, that the stochastic ocean schemes improve the variability there even at depth. The reduced mean state bias in the North Atlantic is a new result: CTRL exhibits the common model bias of a cold North Atlantic (Wang et al. (2014)), which is alleviated in OCE. This bias reduction comes hand in hand with a bias reduction of the North Atlantic jet, as measured using zonal winds at 850hPa: see Figure B1 in Appendix B. The close link between North Atlantic SST biases and the jet have been examined in, e.g., Keeley et al. (2012). Somewhat counter-intuitively, the stochastic schemes generally *decrease* the interannual variability of SSTs. In effect, a small increase in variability is found in the Gulf Stream and Kuroshio regions at all timescales and seasons, with a general decrease elsewhere, especially the equatorial Pacific. The changes in the North Atlantic and Pacific will be revisited again in later sections.

https://doi.org/10.5194/wcd-2021-61
Preprint. Discussion started: 1 October 2021


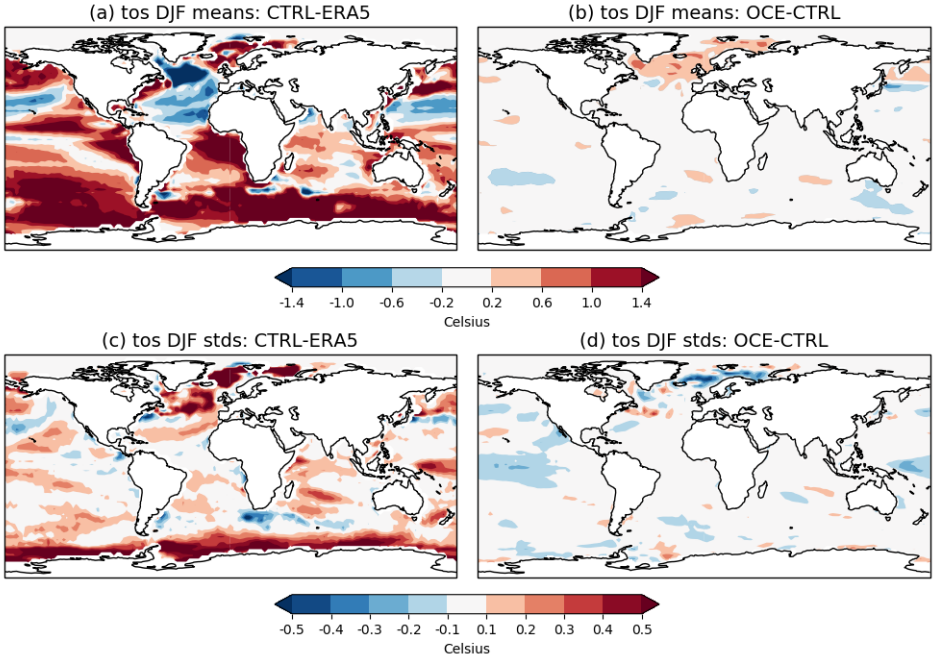


**Figure 3.** Sea surface temperature (mean and standard deviations) in DJF. Mean quantities in (a) CTRL-ERA5 and (b) OCE-CTRL. Standard deviations in (c) CTRL-ERA5 and (d) OCE-CTRL. In each plot, every gridpoint outside the zero contour is significant ($p<0.05$). The period considered is 1980-2015.

Examination of other variables support an overall conclusion that the stochastic sea ice and ocean schemes are having only a moderate impact on the climate mean state, and do not, for example, alter the net surface global energy (not shown). It is likely that this limited impact is due to the fact that the $1^\circ$ ocean does not permit eddies and is strongly damped by viscosity. Consequently, the stochastic ocean schemes, which are primarily attempting to perturb the variability of turbulent processes, cannot achieve much without making the perturbations extreme in magnitude (Juricke et al., 2017). This viewpoint is supported by the fact that in separate experiments using a $0.25^\circ$ ocean, the impact of the same schemes on SST variability was much greater (not shown). The main exception to this is in the Arctic and regions such as the North Atlantic, where, firstly, the sea ice perturbations play an active role, and, secondly, where the interplay between Gulf stream variability, atmosphere-ocean coupling and vertical mixing in the ocean is large enough for the ocean perturbations to have a bigger non-linear mean impact.

## 4 Impact on Arctic-NAO Teleconnections

### 4.1 Identification of the centres of action

We examine the impact of stochasticity on the teleconnections between Arctic sea ice in November and the winter NAO. Studies in the literature often do this by first creating a timeseries of sea ice anomalies for a chosen region, such as Barents-

https://doi.org/10.5194/wcd-2021-61
Preprint. Discussion started: 1 October 2021


Weather and Climate Dynamics Discussions
Open Access
EGU

Kara, and then regressing this against atmospheric variables (e.g., zg500 or sea level pressure) at each gridpoint, or against an NAO timeseries (e.g., Blackport et al. (2019); Koenigk and Brodeau (2017)). However, as shown in the previous section (c.f. Figure 2), the Barents-Kara region emerges as an area of interest in reanalysis data by virtue of being the dominant source of interannual sea ice variability near the North Atlantic. Many studies have made the point that the Barents-Kara region, particularly the Barents sea, acts as a transition zone between the open seas in the south and the permanently ice-covered north (Deser et al. (2000); Vinje (2001); Koenigk et al. (2009)). The strong variability here is therefore largely reflecting variations in where the sea ice edge ends up extending to each winter, with the primary driver being the extent to which anomalous winds transport sea ice into the region from the central Arctic (see, e.g., Koenigk et al. (2009) for a comprehensive overview). The strong temperature gradients between the relatively warm ocean and the cold atmosphere aloft mean that these variations in the extent of the sea ice edge are associated with heat fluxes anomalies reaching as high as $500 W m^{-2}$ (ibid). Because it is these heat flux anomalies that are hypothesised to influence the circulation, as opposed to the sea ice per se, we strongly argue that an examination of Arctic-midlatitude teleconnections using free-running climate model data needs to take into account the fact that models will inevitably drift to their own preferred sea ice edge with their own leading modes of variability. Because of the possible dependency on the mean state (Deser et al. (2007); Strong and Magnusdottir (2010)), model drift in its atmospheric component may also play a role here, due to interactions with the North Atlantic storm track.

To do this, rather than prescribe the sea ice region of interest up front, we specify the NAO as the fixed phenomenon of interest, and then correlate the winter NAO index with (detrended) November sea ice anomalies at every gridpoint of the Arctic. Spatially coherent regions of significant correlations that coincide with the peaks of the sea ice EOF patterns are taken as evidence of a potential teleconnection, which we can then examine further. The result of this process is seen in Figure 4, using both reanalysis and model data covering 1980-2015 as well as model data using the entire period 1950-2015. Both ERA5 and OSI450 show a region of positive correlations in the Barents and Kara seas, as expected, and this region clearly corresponds to one where the first EOF displays a large value. The correlations at these gridpoints are also found to be statistically significant, as opposed to elsewhere. By contrast, the CTRL experiment exhibits no consistent signal in the Barents or Kara sea for either time-period, showing instead a signal near the Bering sea, consistent with the large amplitude of the EOF there. On the other hand, the OCE experiment exhibits a coherent signal in the Barents and Greenland sea in the modern period 1980-2015 (Figure 4e), which both becomes stronger and encompasses a wider region when considering the entire period 1950-2015 (Figure 4f). The Barents sea, and to a lesser extent, the Greenland sea, correspond to regions of high EOF values. Note that, due to the large sample size of 105 years, the correlations are found to be significantly different from 0 at every gridpoint outside the zero contour for CTRL and OCE. The question of statistical significance is addressed in depth in the next section. The reason the signal appears to be bigger and covering a larger region when using the full time-period is likely due to the sea ice loss that occurs between 1950 and 2015 (not shown). Both models lose a considerable amount of sea ice in the Greenland, Barents and Kara seas, with the OCE model losing somewhat less in Barents and Greenland and somewhat more in Kara. The loss of sea ice in the Greenland sea in particular is associated with a permanent retreat of the sea ice edge, and a subsequent loss of any interannual variability there.

https://doi.org/10.5194/wcd-2021-61
Preprint. Discussion started: 1 October 2021


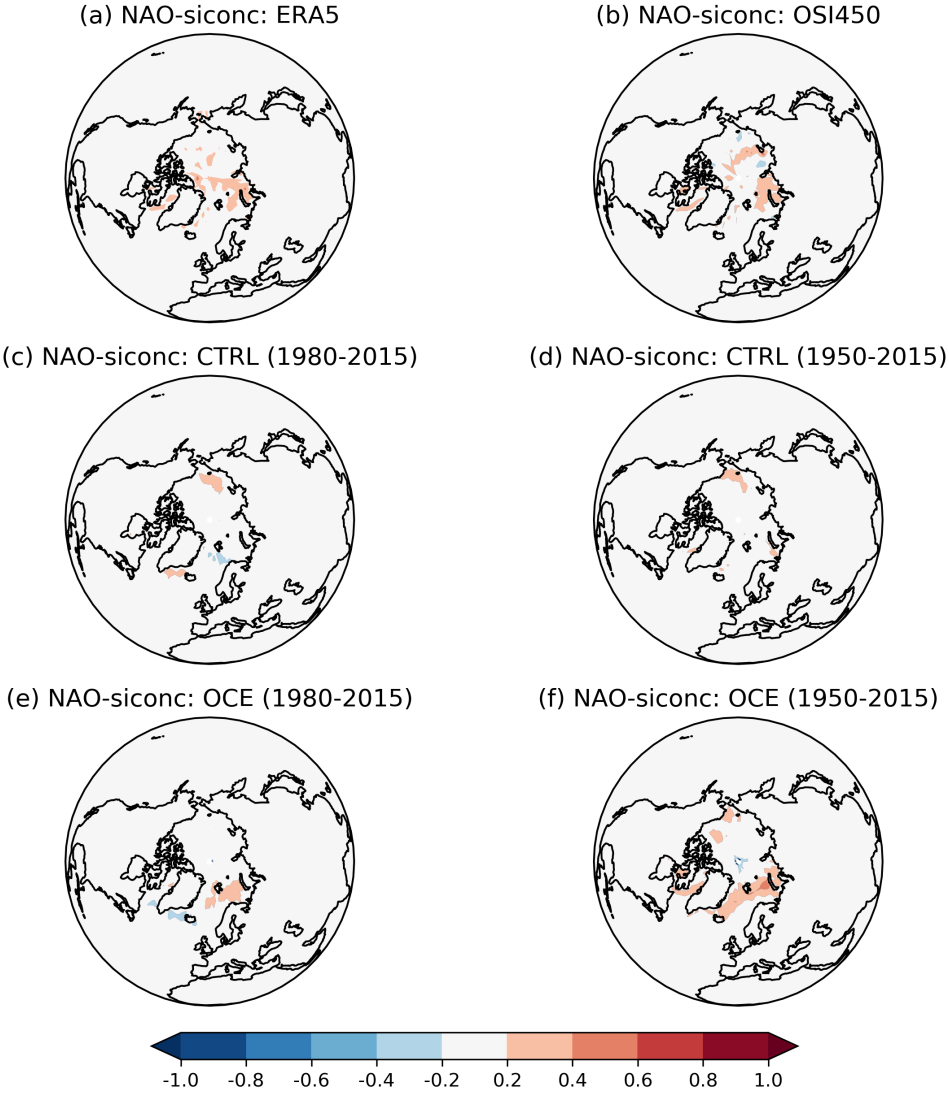


**Figure 4.** Correlations between the detrended November siconc anomalies at each gridpoint and the DJF NAO timeseries. In (a) ERA5 (1980-2015), (b) OSI450 (1980-2015), (c) CTRL (1980-2015), (d) CTRL (1950-2015), (e) OCE (1980-2015), (f) OCE (1950-2015). xThe ensemble members of the CTRL and OCE experiments have all been concatenated together. For the CTRL and OCE plots ((c) through (f)), every gridpoint outside the zero contour is statistically significant ($p < 0.05$). For ERA5 and OSI450, only gridpoints in the Barents and Kara seas are significant.

From these observations we draw the following conclusions. For observational data, the Barents-Kara region clearly stands out as the region where a potential teleconnection link with the NAO may occur. In the OCE model, the centre of action appears shifted west to the Barents-Greenland region, with the importance of Greenland diminishing over time as the sea ice retreats

https://doi.org/10.5194/wcd-2021-61
Preprint. Discussion started: 1 October 2021


| | ERA5 | CTRL | $CTRL_1$ | $CTRL_2$ | $CTRL_3$ | OCE | $OCE_1$ | $OCE_2$ | $OCE_3$ |
|---|---|---|---|---|---|---|---|---|---|
| Raw correlations | **0.39** | -0.13 | -0.09 | -0.10 | -0.23 | **0.29** | 0.30 | 0.21 | **0.37** |
| LIM correlations | **0.37** | -0.14 | -0.11 | -0.10 | -0.19 | **0.23** | 0.26 | 0.23 | 0.31 |

**Table 1.** Correlations between November sea ice anomalies in the BK (resp. BG) region for ERA5 (resp. EC-Earth3 experiments) and the DJF NAO mean, over the period 1980-2015. The "Raw correlations" row contains values estimated using the actual model and reanalysis data, while the "LIM correlations" row contains estimates from the Linear Inverse Model reconstructions (cf Section 5**??**). Subscript labels $CTRL_n$ and $OCE_n$ (N=35) denote ensemble members 1-3, while the entry for CTRL and OCE (N=105) uses the concatenated timeseries. Entries that are significant (p<0.05) are marked in bold. Significance is measured against a null hypothesis of uncorrelated, random AR1 processes.

due to global warming. In the CTRL model, the only notable signal appears to be from the Bering sea. Because this is consistent with the Bering sea being a region of peak variability in CTRL, it is possible that this region should be viewed as the equivalent of 'Barents-Kara' for the deterministic model. While some studies, such as Koenigk et al. (2016), have examined the impact of sea ice from other regions in the Arctic, this is not common, with the majority of studies focusing attention on either the Arctic as a whole or Barents-Kara in particular. In order to keep our analysis aligned with existing studies, and because of both the remoteness of the Bering sea relative to Barents-Kara sea and the lack of such a signal from the Bering sea in observational data, we will not pursue the role of the Bering sea further.

For the remainder of this paper, we will therefore be examining and comparing the teleconnections between the winter NAO and the mean November sea ice anomaly across the following regions:

1. For ERA5: Barents-Kara (BK), defined by the box 67N-80N, 30E-75E.
2. In CTRL/OCE: Barents-Greenland (BG), defined by the box 65N-82N, 5E-60E.

To allow for ease of language, we will sometimes omit the abbreviations BK and BG and simply refer informally to 'the teleconnection', 'the ice-NAO teleconnection', or 'the sea ice', with the implicit understanding that this should be understood in a context-dependent sense.

### 4.2 Assessment of statistical significance

The "Raw correlations" row in Table 1 summarises the correlations between the November sea ice and the winter NAO over the period 1980-2015. To assess the statistical significance of the correlations, a null hypothesis of each timeseries as an $AR(1)$ process is assumed. By fitting such a process to each timeseries and simulating 10,000 random draws, we obtain confidence intervals for the correlations expected by chance. For ERA5 and the individual ensemble members of CTRL and OCE, which have a sample size of 35, a 95% confidence interval is approximately given by $\pm 0.35$. For the concatenated timeseries of CTRL and OCE, which have a larger sample size of $35 \cdot 3 = 105$, the 95% confidence interval is approximately $\pm 0.2$; a 99% interval is given by $\pm 0.24$. Correlations significant to the 95% threshold are shown in bold in Table 1.

https://doi.org/10.5194/wcd-2021-61
Preprint. Discussion started: 1 October 2021


It can be seen that ERA5 exhibits a significant positive correlation of $\approx 0.39$, consistent with that reported by many other studies using a variety of techniques and observational datasets. While every ensemble member of OCE shows a positive correlation, only one is significantly different from 0. However, after concatenation, OCE has a correlation of 0.29, which is even significant at the 99% threshold. By contrast, and as expected from Figure 4, neither individual CTRL members, nor the concatenated data set, shows significant correlations, with all showing a small negative correlation.

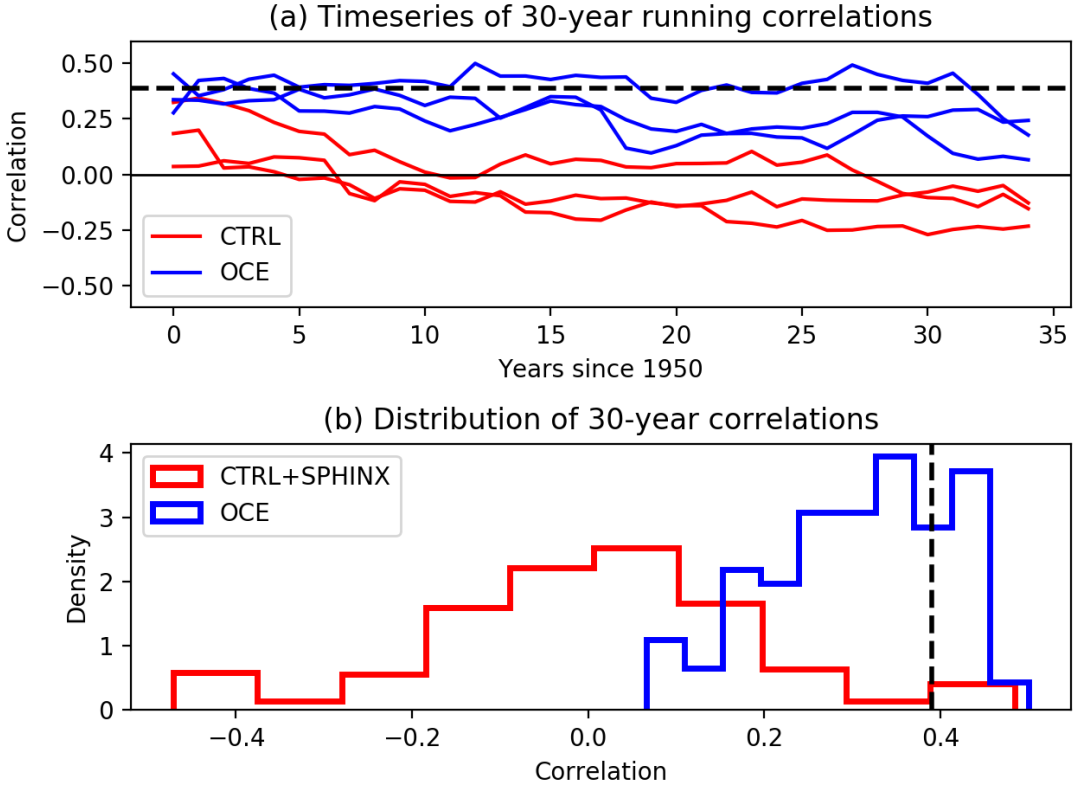


**Figure 5.** In (a), timeseries of the correlations between November sea ice and the DJF NAO across successive 30-year chunks 1950-1980, 1951-1981, ... 1985-2015; for the three CTRL members (red), and the three OCE members (blue). In (b), the distributions of all such 30-year correlations across the CTRL and deterministic SPHINX experiments (red), and the OCE experiments (blue). The stipled black line in both marks the correlation found in ERA5 for the period 1980-2015. The CTRL/OCE experiments cover 1950-2015, while SPHINX covers 1900-2015.

As discussed in the introduction, there remains considerable uncertainty in the literature concerning the robustness of the teleconnection. In particular, it has been suggested that the observed correlation is in fact just a spurious signal arising from decadal variability in the coupled ocean-atmosphere dynamics (Koenigk and Brodeau (2017)). Therefore, while the raw correlations of Table 1 already support a conclusion that the stochastic ocean and sea ice schemes have, at least partially, restored a teleconnection in observations that was missing in the deterministic model, it is appropriate to assess the robustness of this

https://doi.org/10.5194/wcd-2021-61
Preprint. Discussion started: 1 October 2021


result further. To this end, we have plotted, in Figure 5(a), the evolution of ice-NAO correlations across the successive 30-year chunks 1950-1980, 1951-1981, . . . , 1985-2015, for each ensemble member. Note that values inferred from the last data points of this plot will differ somewhat from those of Table 1 due to the shorter 30-year time-periods being considered.

While all the simulations appear to be initialised into a period of positive correlations, the correlations are systematically smaller for CTRL, and after only 5 years all three CTRL members appear to have drifted to a state with no robust teleconnection. None of the CTRL members achieve a correlation as high as that of ERA5 across any 30-year time-period, where we note that the correlations in ERA5 vary roughly from $0.37$ to $0.41$ across the 30-year chunks between 1980 and 2015. The decadal variability in the CTRL correlations also suggests that the slightly negative correlations found in this recent time-period is mostly coincidental, consistent with the lack of statistical significance of these correlations. On the other hand, all three OCE members maintain positive correlations across every chunk, and frequently attain values comparable to ERA5. This implies that the highly significant correlation obtained when concatenating all three members is not just a result of a lucky choice of time-period, but a signal that can be consistently located across the entire simulation period: for each 30-year chunk, the concatenated ensemble members of OCE are found to produce statistically significant correlations.

To further assess the likelihood that the behaviour seen in the OCE experiments is just chance, we can compare the distribution of 30-year OCE correlations with the distribution drawn from a larger sample of deterministic EC-Earth3 experiments, encompassing both CTRL and the deterministic SPHINX experiments (see Section 2). The SPHINX experiments consist of 3 coupled simulations covering the period 1900-2015 with historical forcing, and so boost the sample size by 345 years. The results are seen in Figure 5(b). While the SPHINX members are between themselves able to briefly attain correlations of a magnitude comparable to ERA5, this is evidently a rare event. Indeed, we computed that only $\approx 11\%$ of deterministic 30-year correlations exceed $0.2$. Under the assumption that the three ensemble members of OCE are fully independent of each other, the likelihood of all of them consistently attaining correlations exceeding $0.2$ by chance is therefore less than $0.13\%$. In reality, the assumption of independence is unlikely to be strictly true, since the initial ocean and sea ice state may bias the experiments towards certain decadal trends. However, since the CTRL members fail to manifest similar behaviour, such a dependence between members is likely to be weak, and either way, even if our crude estimate of $0.13\%$ is off by an order of magnitude, the conclusion would still hold that the behaviour of OCE is unlikely to be purely coincidental. We note that the same conclusion was found to hold if we boosted the sample size of deterministic correlations by adding in those observed in the period 1980-2010 across the CMIP6 ensemble (not shown). Indeed, the distributions from CTRL, SPHINX and CMIP6 all appear to be equivalent, ranging between $\pm 0.3$ with a mean of $0$.

We interpret this analysis as supporting the assertion that the teleconnection is significantly stronger in the OCE experiments relative to CTRL, and the remainder of the paper will take this assertion as the starting point for further analysis. In the following sections, the goal of our analysis is to understand in more detail how the teleconnection has changed and why.

https://doi.org/10.5194/wcd-2021-61
Preprint. Discussion started: 1 October 2021


Weather and Climate Dynamics Discussions
Open Access
EGU

## 5 A Quantitative Explanation via Ice-Ocean-Atmosphere Coupling

### 5.1 Mean state changes alone do not suffice

In Section 3 it was shown that the stochastic schemes have notably changed the mean state of North Atlantic SSTs and Arctic sea ice. An obvious first hypothesis is therefore that the improved teleconnection is the result of an improved mean state. To test this, we examined an equivalent set of three deterministic ensemble members using prescribed SST/ice boundary forcing, which we refer to as the AMIP ensemble. The equivalent version of Figure 4 for AMIP (Figure B2), obtained by correlating the model's NAO with the prescribed sea ice at each gridpoint, shows no indication of any ice-NAO link, including the BK or BG region. The correlations of the November BK sea ice anomalies and the DJF NAO, for each of the three ensemble members, are 0.18, 0.01 and -0.05: the correlation using the concatenated timeseries is 0.06. None of these values are significantly different from 0, and considering other 30 or 35-year periods between 1950 and 2015 does not change this.We therefore conclude that the AMIP ensemble does not exhibit an ice-NAO teleconnection. The same conclusion holds when using the BG region instead.

### 5.2 Reconstructing the teleconnection from daily time scale coupling

The fact that prescribing the ocean and sea ice forcing does not result in the deterministic model exhibiting a significant teleconnection implies that a crucial role is being played by the dynamic coupling of the atmosphere and the ocean/ice. The potential importance of coupling to maintain the circulation response associated with Arctic sea ice anomalies was already emphasised in Strong and Magnusdottir (2011). To gain additional insight into this, we examine the temporal evolution of the teleconnection. This is done in Figure 6, which shows the regression coefficients of November BK (resp. BG) sea ice anomalies against monthly zg500 anomalies in November, December and DJF in ERA5 (resp. CTRL and OCE).

The initial November response is fairly similar in all three data sets, with a tripole pattern formed by a low over the Kara sea, a high near Greenland and a low near the eastern coast of North America. In the following months, both ERA5 and OCE see this tripole evolve into a larger low centred on Greenland, with a broad high across the North Atlantic and Europe; in DJF this pattern clearly corresponds to a positive NAO for both. In CTRL, on the other hand, the same evolution never takes place, and seasonal evolution simply consists of a slow dissipation of the initial November response. Because the initial response projects weakly onto the negative NAO, the correlation between November BG sea ice and the winter NAO is often slightly negative, as seen in Figure 5(a). Similar plots showing the initial heatflux anomalies (Fig B3) and the temperature anomaly evolution (Figure B4) corroborate this story, with a similar initial response that evolves more realistically over time in OCE. Note that qualitatively similar results are found if we use the BK region for the CTRL experiments.

The ability of OCE to evolve the same initial response better than CTRL might be plausibly attributed to changes in persistence, either of the NAO or the sea ice. However, since the atmospheric component is identical in OCE and CTRL, there is no obvious mechanism for how the persistence of the NAO might change, and the lack of a teleconnection when prescribing the sea ice rules out the persistence timescales of the sea ice alone from explaining the change. Figure B5 confirms that the daily autocorrelation of the NAO has not changed notably between OCE and CTRL; both OCE and CTRL have much higher sea ice persistence than ERA5, but again, the difference between OCE and CTRL is small. By contrast, Figure 7 shows a marked dif-

https://doi.org/10.5194/wcd-2021-61
Preprint. Discussion started: 1 October 2021


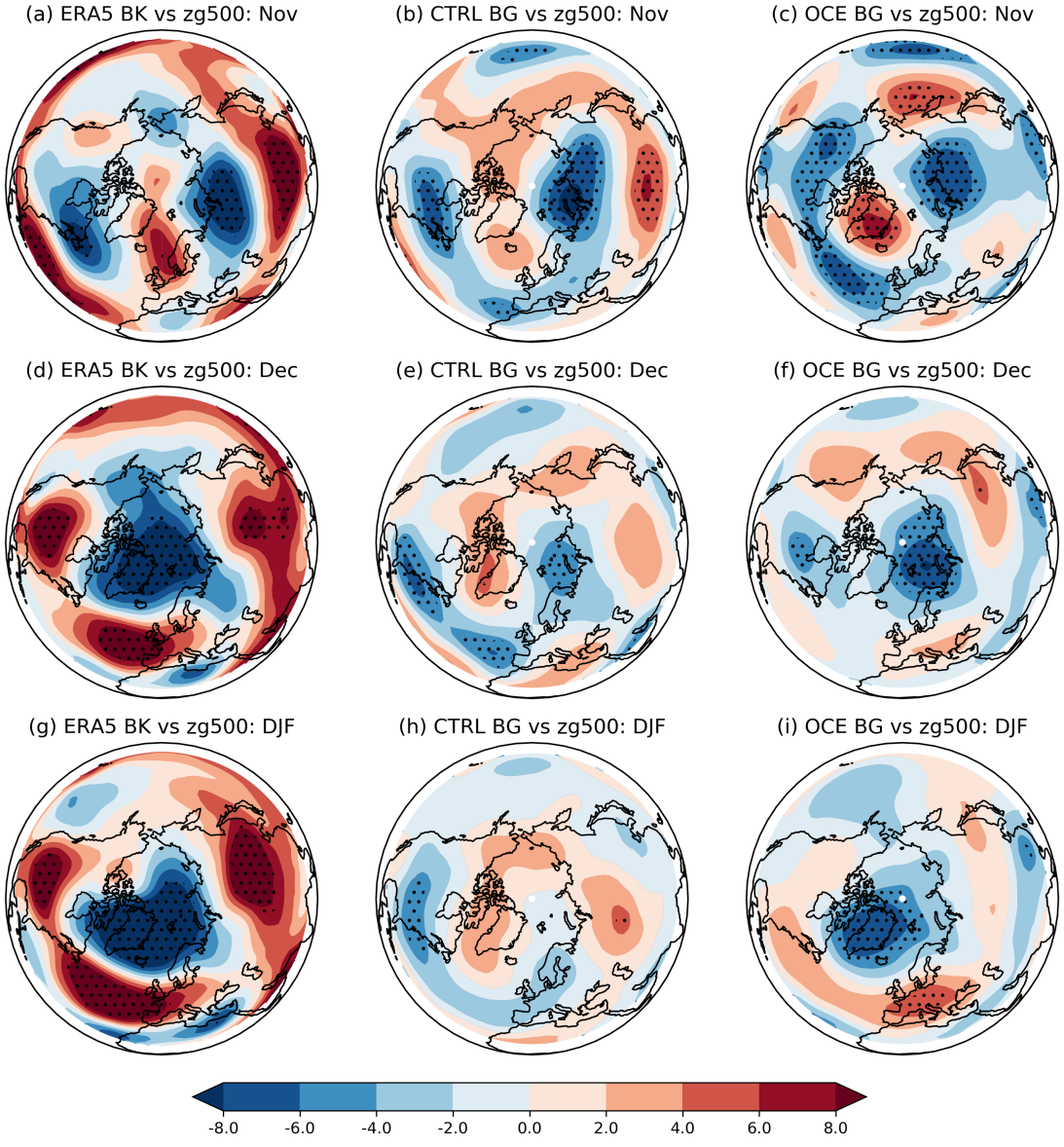


**Figure 6.** Regression coefficients of November BK sea ice anomalies against monthly zg500 gridpoint anomalies in ERA5 for (a) November, (d) December and (g) DJF. The same for CTRL (resp. OCE) in (b), (e) and (h) (resp. (c), (f) and (i)), but with BG sea ice used instead. The period considered is 1980-2015. Stipling highlights gridpoints where the associated correlation coefficient is statistically significant ($p < 0.05$).

375 ference between OCE and CTRL in the cross-correlation. While there is no clear difference between observations and models in the cross-correlation when the NAO leads the sea ice, the OCE model appears to be considerably more realistic when the sea ice leads the NAO, with CTRL showing virtually no impact of sea ice on the NAO whatsoever. Note that the opposite signs of

https://doi.org/10.5194/wcd-2021-61
Preprint. Discussion started: 1 October 2021


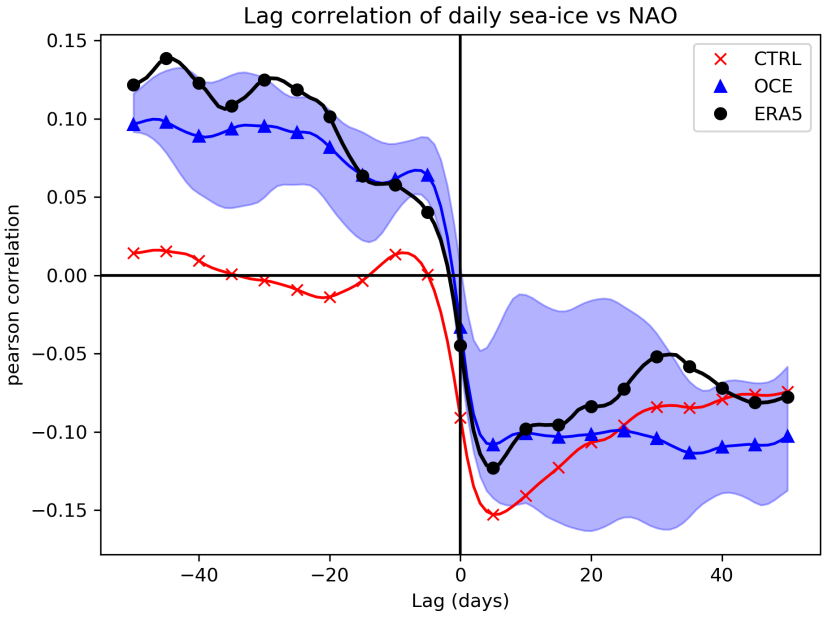


**Figure 7.** Lagged correlations of the daily NAO against the daily BK (resp. BG) sea ice for ERA5, black dotted (resp. CTRL, red crosses, and OCE, blue triangles). Negative lags correspond to sea ice forcing the NAO, and vice versa for positive lags. Data is restricted to days in November through February, 1980-2015. Shading indicates the ensemble spread of OCE: the CTRL spread (not shown) is similar in extent.

the cross-correlation based on whether the ice or the NAO is leading suggests a natural physical interpretation of the coupling. A positive sea ice anomaly in the BK or BG region (i.e., an extension of the sea ice edge) leads to a reduced local heatflux into the atmosphere, which, via a combination of Rossby wave forcing and changes to the meridional temperature gradient, force the positive phase of the NAO. This corresponds to a northward shift of the eddy-driven jet (Woollings et al. (2010)), which would lead to anomalous wind stress in the BK (or BG) region and a consequent reduction of the initial positive sea ice anomaly. The importance of wind forcing was emphasised in Koenigk et al. (2009). The more northerly jet may also lead to shifts in the sea ice more broadly which are potentially important to support a realistic evolution of the initial atmospheric response.

In order to test if the change in daily coupling between the ice and the NAO can account for the changes in the teleconnection, we model the system using the following pair of coupled ordinary differential equations:

$$\frac{d}{dt}\mathrm{NAO} = a \cdot \mathrm{NAO} + b \cdot \mathrm{ICE} + \xi_{\mathrm{NAO}}, \tag{1}$$

$$\frac{d}{dt}\mathrm{ICE} = c \cdot \mathrm{NAO} + d \cdot \mathrm{ICE} + \xi_{\mathrm{ICE}}. \tag{2}$$

Here NAO is just the daily NAO index, and ICE is the daily sea ice anomaly in either BK or BG depending on the data set. The coefficients $a$ and $d$ are capturing the presence of autocorrelation, while the coefficients $b$ and $c$ capture the presence of coupling; the $\xi$ terms in both equations represent the residual forcing on both quantities, and are assumed to be random

https://doi.org/10.5194/wcd-2021-61
Preprint. Discussion started: 1 October 2021


Gaussian processes with no temporal autocorrelation and a mean of 0. This model (hereafter referred to as the LIM), has been used extensively in the literature to capture coupled variables in climate data, such as atmosphere-ocean coupling, and the coefficients and noise terms can be estimated using Linear Inverse Modeling (see, e.g. Penland and Sardeshmukh (1995); Penland and Magorian (1993); Alexander et al. (2008); Hawkins and Sutton (2009); Newman et al. (2009) for some examples). A brief summary of how to do this is included in Appendix A: the reader may consult Penland and Sardeshmukh (1995) for more details. We are not aware of earlier examples in the literature applying the LIM framework to ice-atmosphere coupling, though the approach of Strong and Magnusdottir (2011) is closely related.

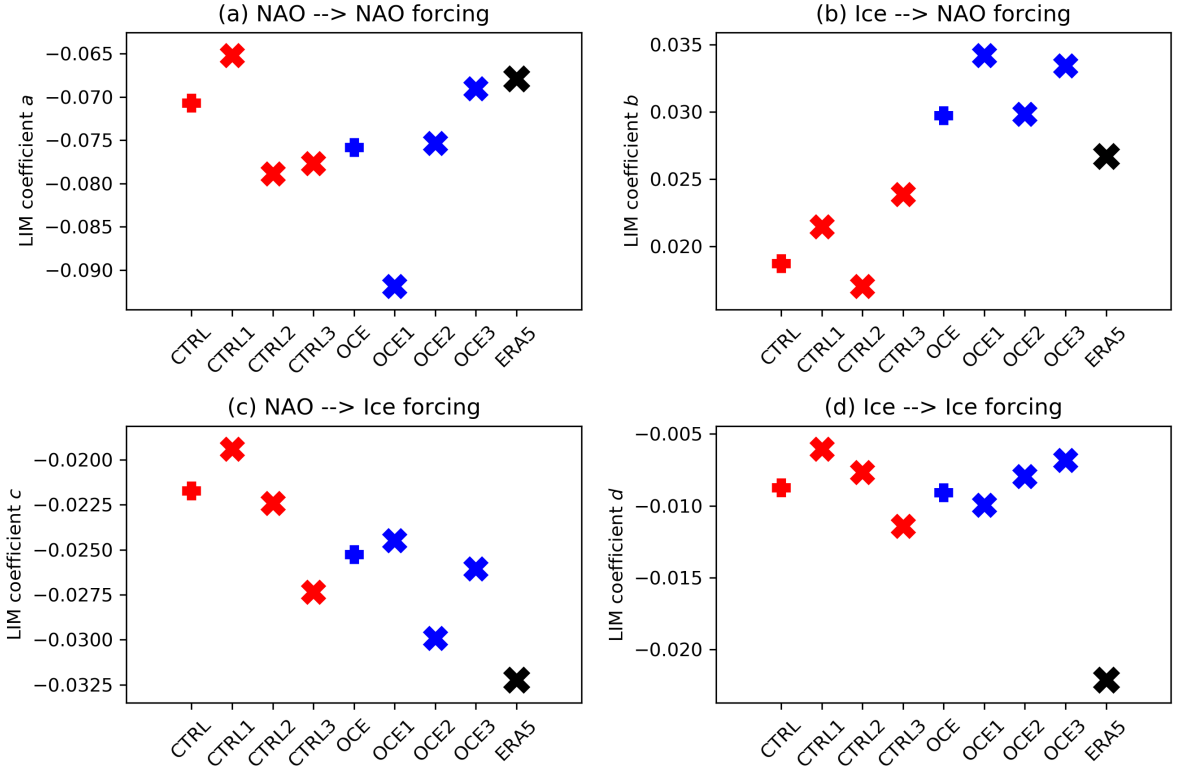


**Figure 8.** Estimated coefficients of the LIM model, as described by equations (1) and (2). In (a): the coefficient $a$, describing the forcing of the NAO on itself one day later; (b) the coefficient $b$, describing the forcing of sea ice on the NAO one day later; (c) the coefficient $c$, describing the forcing of the NAO on sea ice one day later; (d) the coefficient $d$, describing the forcing of sea ice on itself one day later. CTRL (resp. OCE) data is marked in red (resp. blue), with crosses used for ensemble members and plus signs for the concatenated data. ERA5 is shown with a black cross. Daily data covering November-February, 1980-2015, is used.

Figure 8 shows the estimated LIM coefficients for ERA5 (black), CTRL (red) and OCE (blue), where daily data spanning November through February (NDJF) of 1980-2015 has been used. Fitting the LIM requires a choice of a lag, and we used the simplest possible choice of 1 day. Using these coefficients and the November initial conditions for each data set, it is straight

https://doi.org/10.5194/wcd-2021-61
Preprint. Discussion started: 1 October 2021


Weather and Climate Dynamics Discussions
Open Access
EGU

forward to generate a reconstruction of the daily NDJF data using the LIM (see Appendix A for details). To assess the accuracy of the LIM, we created such reconstructions of the NDJF sea ice and NAO for ERA5, each model ensemble member, and for the concatenated data sets of CTRL and OCE. The correlations between the reconstructed DJF NAO and the true DJF NAO are listed in the second row of Table 1. Comparison with the first row suggests the LIM has, to a large extent, reproduced the observed correlations for all the data sets: plots of the reconstructions are shown in Figure B6 of the SI. In other words, the seasonal timescale teleconnection appears to be explainable using only information about daily timescale coupling and initial conditions.

Having thus confirmed the LIM's ability to reproduce the teleconnection to good accuracy, we may with some confidence examine the variations in the coefficients seen in Figure 8. Two obvious features stand out. Firstly, all EC-Earth3 data experiments have a $d$ coefficient which is too small (Figure 8d), which corresponds precisely to their overly high sea ice autocorrelation (Figure B5). Secondly, the coupling coefficients $b$ and $c$ are closer to ERA5 in the OCE experiments compared to CTRL, especially for the $b$ coefficient. The larger $b$ coefficient in particular corresponds to the increased daily lag-correlation between sea ice and the NAO seen in Figure 7. As a final note, little difference was found in the estimated magnitude of the noise terms $\xi_{\text{NAO}}$ and $\xi_{\text{ICE}}$ across CTRL and OCE, though the latter was found to be smaller in magnitude compared to ERA5. This is consistent with the overly high autocorrelation in modelled sea ice (Figure B5).

To conclude, analysis of the LIM model suggests that the teleconnection (or lack thereof) in each data set considered can be accounted for from daily timescale coupling alone, and that the strength of the coupling is quantitatively stronger in OCE than in CTRL. If one collapses the coupling coefficient $b$ to 0 (not shown), the LIM fails to reconstruct the observed correlations for OCE and ERA5, which supports the hypothesis that this coupling is a crucial component of the teleconnection.

## 6 Alternative Hypotheses

We now consider three alternative hypotheses for why the observed teleconnection may have changed: unforced internal atmospheric variability, changes in tropical forcing, and changes in the atmosphere-ocean coupling in the North Atlantic.

### 6.1 The role of internal atmospheric variability

It has been argued that the observed teleconnection may, to a large extent, be driven by (possibly chaotic) atmospheric variability. To assess if this is playing a role here, we will use the framework of Blackport et al. (2019). For each November between 1980 and 2015, the signs of the average ocean heatflux (latent+sensible) and sea ice anomalies across the month are examined; denote these by $S_{flux}$ and $S_{ice}$ respectively. Note the heatflux sign-convention is taken such that a positive sign corresponds to a net flux up into the atmosphere. Physical reasoning justifies the following classification: November months with $\{S_{flux} > 0, S_{ice} < 0\}$, or $\{S_{flux} < 0, S_{ice} > 0\}$ are classified as ones where the sea ice is forcing the atmosphere. Similarly, November months with $\{S_{flux} < 0, S_{ice} < 0\}$, or $\{S_{flux} > 0, S_{ice} > 0\}$ are classified as ones where the atmosphere is forcing the sea ice. By restricting to these two disjoint subsets of years, one can assess which class of winters contribute the most to the teleconnection.

https://doi.org/10.5194/wcd-2021-61
Preprint. Discussion started: 1 October 2021


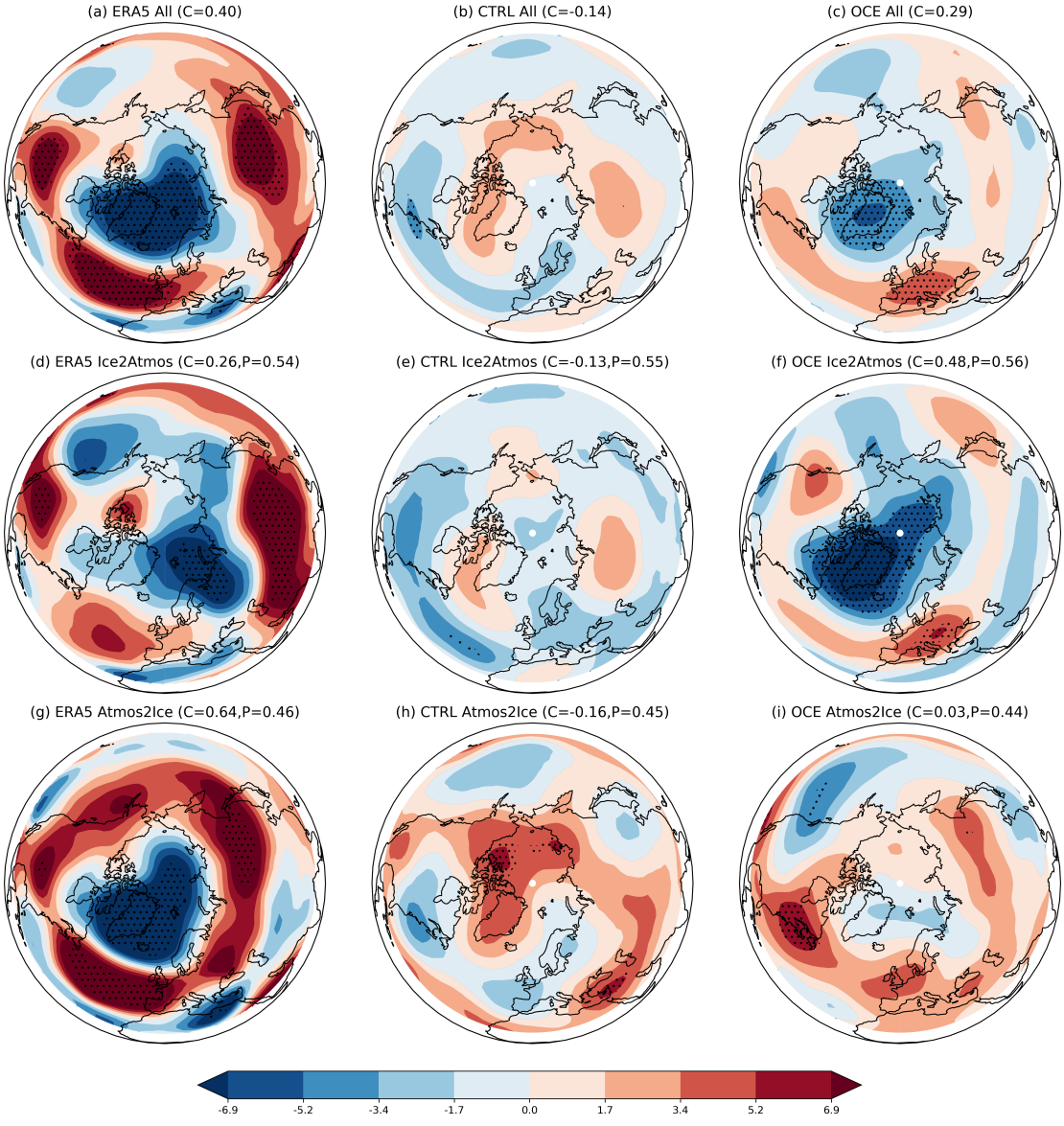


**Figure 9.** Regression coefficients between November BK (resp. BG) sea ice anomalies and DJF zg500 anomalies for ERA5 (resp. CTRL and OCE). In (a) all years, (d) years where the ice drives the atmosphere and (g) years where the atmosphere drives the ice. In (b), (e) and (h): the same but for CTRL. In (c), (f) and (i): the same but for OCE. The value of $C$ in the headers is the correlation between the sea ice timeseries and the DJF NAO index when restricted to those years. The value $P$ is the proportion of years falling into the given category for that data set. The period used is 1980-2015. Stipling highlights gridpoints where the associated correlation coefficient is statistically significant ($p < 0.05$).

435 The result of this process for ERA5, CTRL and OCE is shown in Figure 9. The first column ((a), (d) and (g)) reproduces the result of Blackport et al. (2019) for ERA5, and shows that while both classes of winter manifest a positive correlation between

https://doi.org/10.5194/wcd-2021-61
Preprint. Discussion started: 1 October 2021


November sea ice and the DJF NAO, this correlation is stronger when the atmosphere is driving the ice (0.64 vs 0.26). The second column ((b), (e) and (h)) shows the decomposition in CTRL. There is no strong or coherent projection onto the NAO in either subset, with the biggest signal being a positive anomaly around the Bering Sea in years where the atmosphere drives the ice. This may be related to the concentration of the CTRL sea ice EOF in this region (Figure 2). The third column ((c), (f) and (i)) shows the result for OCE. As in ERA5, both subsets project positively onto the NAO, but the entirety of the overall teleconnection appears to be accounted for by years where the sea ice is driving the atmosphere. In these years, OCE shows a correlation of almost 0.5 between November BG sea ice and the DJF NAO, primarily driven by the considerable negative pressure anomaly extending across Greenland. We note that the proportion of years spent in each of the two subsets is almost identical across all three data sets, implying that the results have not been contaminated by any spurious, non-linear effects (e.g., due to changes in the mean sea ice cover).

The fact that the teleconnection in OCE arises almost entirely from forcing of the sea ice on the atmosphere is consistent with the results of both the LIM and lag-correlation analysis, which suggested that the primary difference between CTRL and OCE was in the daily timescale forcing of sea ice on the NAO. We take this as strong evidence for the hypothesis that changes in the teleconnection are driven by the local impact of stochasticity on the surface coupling, as opposed to random, atmospheric variability unrelated to the stochastic schemes. Because in ERA5 the signal is dominated by years where the atmosphere drives the sea ice, and the opposite happens in OCE, it is possible that OCE may be getting 'the right answer for the wrong reasons', and its sea ice forcing is actually unrealistically strong. However, since the daily timescale forcing in OCE closely matches that in ERA5, this is not obvious. It may rather be that the difference seen between the two subsets of years in ERA5 is partially due to chance, and/or that there is some additional source of predictable atmospheric forcing which is present in ERA5 but not in OCE (e.g., from the stratosphere).

### 6.2 The role of tropical forcing

The results of the previous Section 6.1 already indicate a limited role for external atmospheric forcing, including that originating in the tropics. However, it has been argued that the sea ice induced anomalous wave may require favourable atmospheric conditions, such as a favourable storm track, in order to grow, and such conditions may be influenced by the tropics. Additionally, it is possible that the sea ice state in November is influenced by some preceding or concurrent tropical forcing. In order to check for such potential links, we correlated October (resp. November) gridpoint SSTs with the BK/BG sea ice timeseries (resp. DJF NAO index) for each data set. The results are shown in Figure 9.

While ERA5 shows some signs of a weak link between October ENSO and the November sea ice, this is not present in either CTRL or OCE. The only consistent signal between all three data sets is the expected local link between SSTs and sea ice. In terms of the DJF NAO, ERA5 and OCE both share a signal around the BK/BG region, consistent with the sea ice teleconnection, but otherwise have no common signals. CTRL, on the other hand, exhibits a significant link between the DJF NAO and tropical SSTs covering the ENSO region and extending out to the Indian Ocean. This link is not present either in ERA5 or OCE. The fact that deterministic models may sometimes exhibit dynamics that are too strongly driven by ENSO has been noted previously, and stochastic physics schemes have been shown to alleviate this (Strømmen et al. (2017)). The

https://doi.org/10.5194/wcd-2021-61
Preprint. Discussion started: 1 October 2021


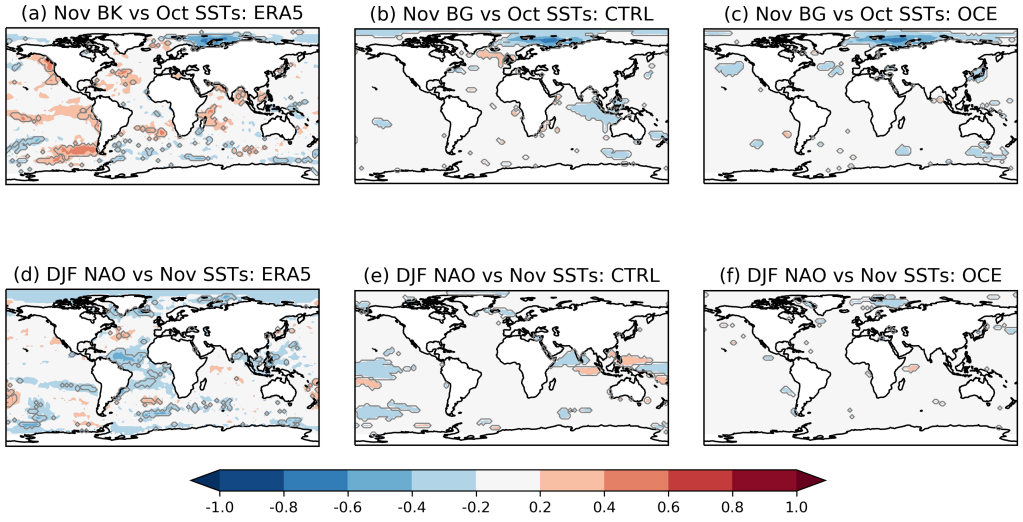


**Figure 10.** Correlations between the detrended October SST anomalies at each gridpoint and the November BK, resp. BG, timeseries for (a) ERA5, resp. (b) CTRL and (c) OCE. Correlations between the detrended November SST anomalies at each gridpoint and the DJF NAO timeseries for (d) ERA5, (e) CTRL and (f) OCE. The ensemble members of the CTRL and OCE experiments have all been concatenated together. The period covered is 1980-2015. The grey contour highlights statistically significant correlations ($p < 0.05$).

removal of this unrealistic signal in OCE appears to be another incarnation of this. While it may seem plausible that this excessive ENSO signal is contributing to an obscuring of an underlying ice-NAO teleconnection in CTRL, we found that the AMIP simulations do not show such an ENSO-NAO link (not shown), and yet still do not exhibit an ice-NAO teleconnection. So, while the removal of this signal in OCE is a clear improvement, it appears to be mostly unrelated to the ice-NAO link.

### 6.3 The role of North Atlantic ocean coupling

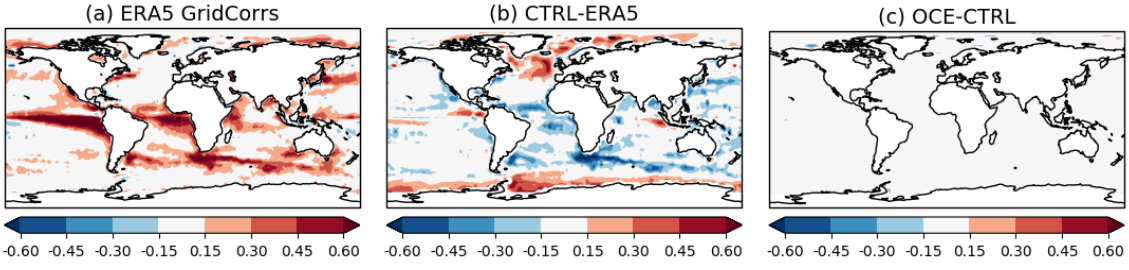


**Figure 11.** Gridpoint correlations between monthly SST anomalies and monthly heatflux anomalies for (a) ERA5, (b) CTRL minus ERA5, and (c) OCE minus CTRL. The period 1980-2015 is used.

https://doi.org/10.5194/wcd-2021-61
Preprint. Discussion started: 1 October 2021


Finally, we considered the possibility that the coupling between the atmosphere and the ocean in, e.g., the North Atlantic, has improved, which might be expected to influence NAO variability. To assess possible changes in atmosphere-ocean coupling, we followed a common methodology (Frankignoul et al. (1998); Von Storch (2000)) of correlating monthly SST anomalies with monthly heatflux anomalies at every gridpoint. The result is shown in Figure 11. Figure 11(b) shows that the CTRL model has several common biases in the coupling, including the tropics and North Atlantic. But from (c) it appears as if OCE is having virtually no impact on these biases. This is in contrast to the impact on the sea ice coupling, as measured using the LIM, where the stochastic schemes lead to a coupling magnitude comparable to ERA5. It is possible that there may be more substantial changes in the coupling occurring on timescales shorter (or longer) than the monthly timescale, but Figure 10 suggests that North Atlantic SSTs have little to no impact on the NAO either way. Therefore, we consider it unlikely that changes to North Atlantic SST variability is making a notable contribution to the altered teleconnection.

## 7 Discussion and Conclusions

We briefly summarise the results of our analysis.

- The inclusion of stochasticity to the ocean and sea ice components of EC-Earth3, as evaluated with the OCE ensemble experiments, leads to the emergence of a statistically significant teleconnection between November Barents-Greenland sea ice and the DJF NAO, comparable to that observed with Barents-Kara sea ice in ERA5. No such teleconnection is present in the deterministic EC-Earth3 (the CTRL ensemble; Table 1).
- The shift in the region of interest from Barents-Kara to Barents-Greenland in OCE is consistent with its differing sea ice EOF: in ERA5 the November variability is concentrated in Barents-Kara, while in OCE it is concentrated in Barents-Greenland (Figure 2).
- Comparison with a large sample of deterministic EC-Earth3 simulations suggests that the odds of generating three random OCE ensemble members which, by chance, all show a consistent ice-NAO teleconnection, is very low (Figure 5).
- An ensemble of deterministic simulations with prescribed sea ice and SSTs is still not able to manifest an ice-NAO teleconnection, implying that the relevant model biases are related to coupling at the surface.
- Analysis using cross-correlations and a simple LIM model suggests that the teleconnections (or lack thereof) in ERA5, CTRL and OCE can all be reconstructed using estimates of daily timescale ice-atmosphere coupling. OCE is found to significantly improve this daily coupling up to a level comparable to that estimated in ERA5 (Figures 7 and 8).
- Splitting the data into years where the ice drives the atmosphere and years where the atmosphere drives the ice (as in Blackport et al. (2019)) shows that the teleconnection in OCE is primarily accounted for by years when the ice drives the atmosphere, suggesting that the change is not simply due to random, internal atmospheric variability (Figure 9).

https://doi.org/10.5194/wcd-2021-61
Preprint. Discussion started: 1 October 2021




– Changes due to the stochastic ocean scheme in the mean state at the ocean surface are small and restricted primarily to the Gulf Stream and Kuroshyo regions, neither of which clearly influence the winter NAO in CTRL or OCE. Similarly, we do not find any clear evidence that changes in tropical SST forcing is having an impact on the ice-NAO teleconnection (Figures 10 and 11).

These results have important implications for the study of Arctic-midlatitude teleconnections, by highlighting the importance of realistic sea ice-ocean-atmosphere coupling. While there is a wealth of literature on atmosphere-ocean coupling, less attention appears to have been paid to coupling involving also the sea ice, with a few notable exceptions, such as Strong and Magnusdottir (2011). Our work supports their conclusion that realistic coupling may be crucial to obtain a realistic teleconnection, and furthermore makes it clear that one cannot expect, a priori, that a given climate model does have realistic coupling. It is therefore possible that some of the inconsistency across different models (Blackport and Screen (2021)), and within long simulations of a single model (Koenigk and Brodeau (2017)), is due to varying model biases in sea ice-ocean-atmosphere coupling. It is also possible that the signal-to-noise paradox in seasonal forecasting is partially due to such biases. The importance of coupling also implies that considering simulations with prescribed boundary conditions, the obvious 'remedy' to the complexities arising from coupled models all having distinct modes of sea ice variability, may not suffice, as the loss of coupling may counteract any gains from a perfect sea ice state. We note that Blackport and Screen (2021) do in fact find that simulations using prescribed boundary conditions exhibit weaker teleconnections than simulations using coupled models.

While the most direct interpretation of our analysis seems to be that stochasticity has altered the surface coupling, we cannot fully rule out the role of mean state changes. This is due to the potential sensitivity of the sea ice signal to a favorable storm track, which implies that getting the right signal may depend on the combined sea ice, ocean, and atmospheric mean state. As such, the lack of a teleconnection in the AMIP experiments does not conclusively rule out that the mean state changes in OCE (Section 3) are crucial. The analysis of lagged correlations and the LIM model lend support to the role of coupling, but it might be that the mean state of OCE is simply better able to propagate a signal which is otherwise identical to CTRL, and that the changes seen in Figures 7 and 8 are simply reflecting this. Untangling this would likely require more careful analysis of shorter, targeted experiments.

If the stochastic schemes are, in fact, improving the coupling between sea ice, ocean, and the atmosphere, what is the precise mechanism which makes the perturbations have this impact? Here too, more careful analysis would be required which goes beyond the scope of this paper. However, a simple conceptual hypothesis might be the following. The evolution of the deterministic sea ice, including how it responds to atmospheric forcing, may be overly 'regular'. Years where the sea ice forces the NAO may depend sensitively not just on the initial sea ice anomaly, but also on how the sea ice then adjusts due to the initial atmospheric response. The deterministic model may simply be confidently doing these adjustments wrong, with the role of stochasticity being to force the model to not always do the same thing. We note that this idea of stochasticity acting as 'damage mitigation' against over-confident deterministic models is ubiquitous in weather forecasting (Palmer et al. (2009); Berner et al. (2017)). That the stochastic sea ice scheme can lead to very different mean responses for Arctic sea ice due to the coupling response with the atmosphere has been shown by Juricke et al. (2018) with dedicated full and one-way coupling experiments.

https://doi.org/10.5194/wcd-2021-61
Preprint. Discussion started: 1 October 2021


Weather and Climate Dynamics Discussions
Open Access
EGU

Our analysis has some important limitations. When it comes to assessing the robustness of the teleconnection in OCE, there is no substitute for a larger ensemble size, and we cannot exclude the possibility that the experiments we considered are biased in some way, e.g. due to the initial conditions predisposing OCE towards certain patterns of decadal variability. Another limitation is that the stochastic schemes considered have only been tested in the context of these teleconnections using a single climate model, and may not produce similar effects in other models. However, the consistency across a range of different types of analysis lends confidence to the hypothesis that the improved teleconnection is not just due to chance. In particular, both the LIM analysis and the methodology of Blackport et al. (2019) provide separate lines of evidence for the change being a result of local sea ice processes. An obvious additional point is that the schemes were introduced precisely to improve variability and coupling (Juricke et al. (2013); Juricke and Jung (2014); Juricke et al. (2014, 2017)), so there is good reason a priori to expect such changes to manifest in experimental data.

Our results, which suggest that the inclusion of a stochastic component in the sea ice and ocean can alleviate model biases, both in coupling, the mean state and variability, adds to an increasingly large body of work showing that stochasticity can be beneficial in models across all timescales. It is especially noteworthy, that although changes to the mean and variability of the model due to stochasticity in this study may, in some regions, be rather moderate, other important physical mechanisms in the climate system, such as teleconnections, might be better represented with the stochastic schemes. It is likely that the stochastic sea ice scheme is the dominant factor for changes to the sea ice-NAO teleconnection seen here, but we note that the study Juricke et al. (2018) has shown that the stochastic ocean schemes can also lead to improved skill over North America in seasonal forecasts, a teleconnection effect they relate to improved ocean-atmosphere coupling. While the use of stochasticity in the atmospheric component is becoming more widespread, its inclusion in other components of the model is still novel. The potential benefits of representing uncertainty in all major components of a climate model was first raised in Palmer (2012), and our paper adds further weight to this view.

*Data availability.* The data is publicly available on Zenodo, via the DOI https://doi.org/10.5281/zenodo.5256102.

NOTE FOR REVIEWERS/EDITORS: The Zenodo data is currently 'Closed Access', but this would be changed to 'Open Access' upon the acceptance of the manuscript. The data can be made available to reviewers prior to this upon request.

## Appendix A: Linear Inverse Modelling

A system of coupled ordinary differential equations, defined by equations (1) and (2), is used to describe coupled ice-NAO interactions on daily time-scales. The parameters are fitted using standard methods of linear inverse modelling. Detailed descriptions of how to do this in full generality can be found in [45] and [44], but to aid the reader we briefly outline the computational steps. Let $B = \left(\begin{smallmatrix} a & b \\ c & d \end{smallmatrix}\right)$ be the coefficient matrix, and let $x$ be the vector made up of the daily time-series of the NAO and ICE. To estimate $B$ in terms of daily time-scale coupling, we computed the lag-0 covariance matrix $C_0$ and the lag-1

https://doi.org/10.5194/wcd-2021-61
Preprint. Discussion started: 1 October 2021


covariance matrix $C_1$ of $x$. The matrix $B$ was then estimated as the matrix logarithm $B = log(C_1 C_0^{-1})$. The noise terms can then be estimated by computing the eigenvectors and values of the 'noise matrix' $Q = -1 \cdot (BC_0 + C_0 B^T)$.

Once the parameters have been fitted in this way for a given data set, a reconstruction of a daily DJF NAO time series can then be created, for a given year, by initializing the coupled system with the NAO and ICE anomalies of November 1st of that year and integrating the system forward in time. We generated, in this way, a perfect deterministic reconstruction of the period 1980-2015 for each data set by suppressing the noise terms: this corresponds to the ensemble mean reconstruction over an infinitely large ensemble. To create the time series of Figure B6 a scaling factor was deduced by creating 1000 explicit simulations (with the noise terms included) and measuring the average standard deviation across these stochastic reconstructions; the deterministic reconstruction was then re-scaled to have this standard deviation. The timeseries thus obtained amounts to what the ensemble mean would look like if it were realized as a stochastic instance. Note that the correlations computed in Table 1 are obviously insensitive to such a re-scaling.

## Appendix B

We include some Figures left out of the main text.

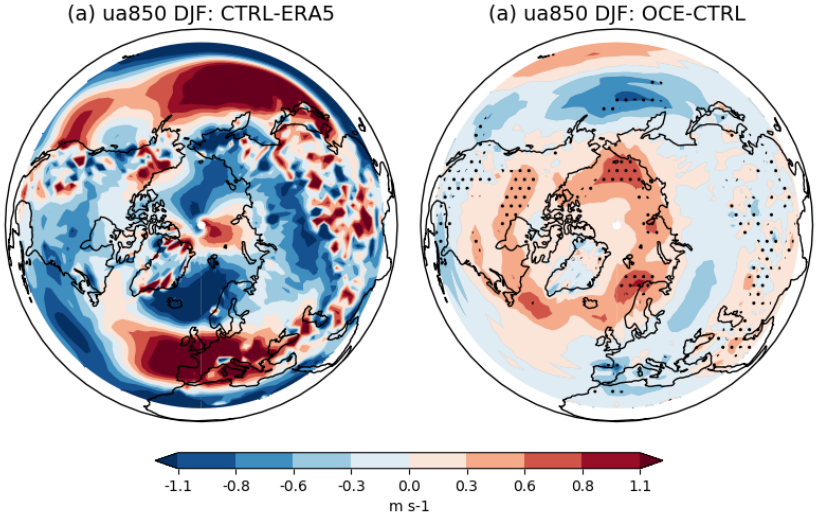


**Figure B1.** Mean zonal winds at 850hPa (ua850) over the DJF season. In (a) CTRL minus ERA5, (b) OCE minus CTRL. Stipling highlights gridpoints where the change is statistically significant ($p < 0.05$); in (a) most points outside the zero contour are significant so stipling is not included for visual ease. The period covered is 1980-2015.

https://doi.org/10.5194/wcd-2021-61
Preprint. Discussion started: 1 October 2021


Weather and Climate Dynamics Discussions
Open Access
EGU

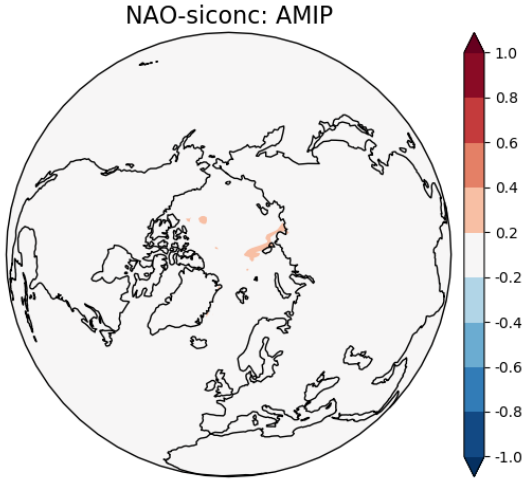


**Figure B2.** Correlations between the detrended November siconc anomalies at each gridpoint and the DJF NAO timeseries, using the AMIP ensemble. All three members have been concatenated. The period covered is 1980-2015.

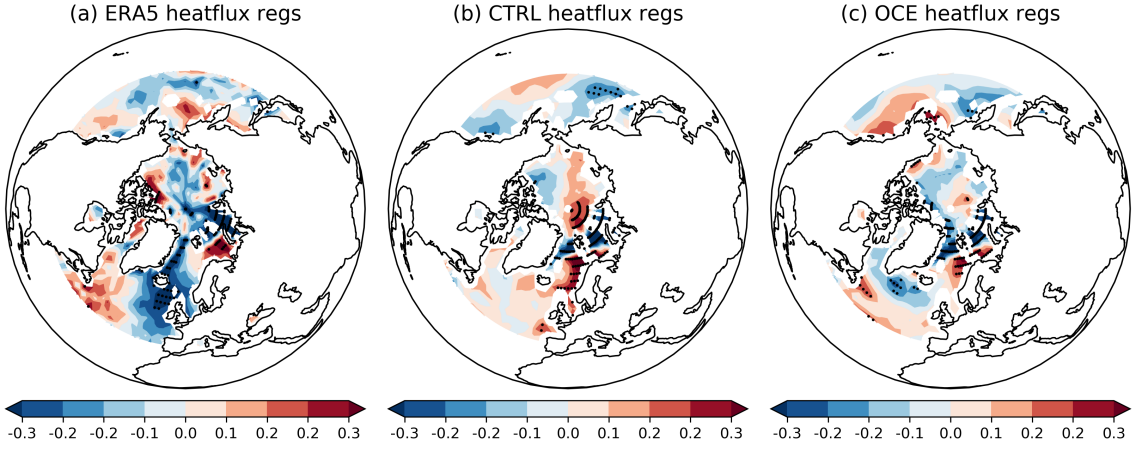


**Figure B3.** Regression coefficients of November BG sea ice anomalies against November heatflux anomalies for (a) ERA5, (b) CTRL, (c) OCE. The period considered is 1980-2015. Stipling highlights gridpoints where the associated correlation coefficient is statistically significant ($p < 0.05$).

https://doi.org/10.5194/wcd-2021-61
Preprint. Discussion started: 1 October 2021


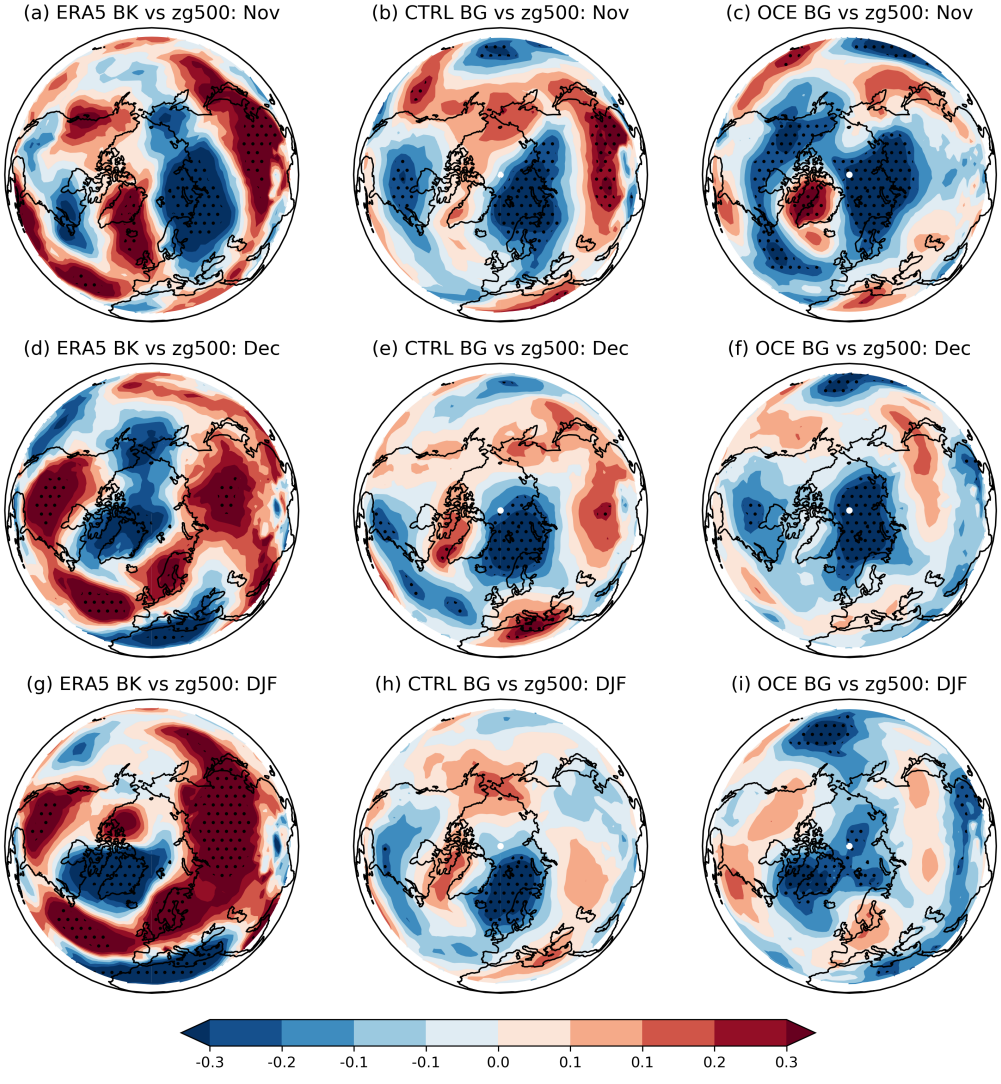


**Figure B4.** Regression coefficients of November BK sea ice anomalies against monthly ta850 gridpoint anomalies in ERA5 for (a) November, (d) December and (g) DJF. The same for CTRL (resp. OCE) in (b), (e) and (h) (resp. (c), (f) and (i)), but with BG sea ice used instead. The period considered is 1980-2015. Stipling highlights gridpoints where the associated correlation coefficient is statistically significant ($p < 0.05$).

https://doi.org/10.5194/wcd-2021-61
Preprint. Discussion started: 1 October 2021


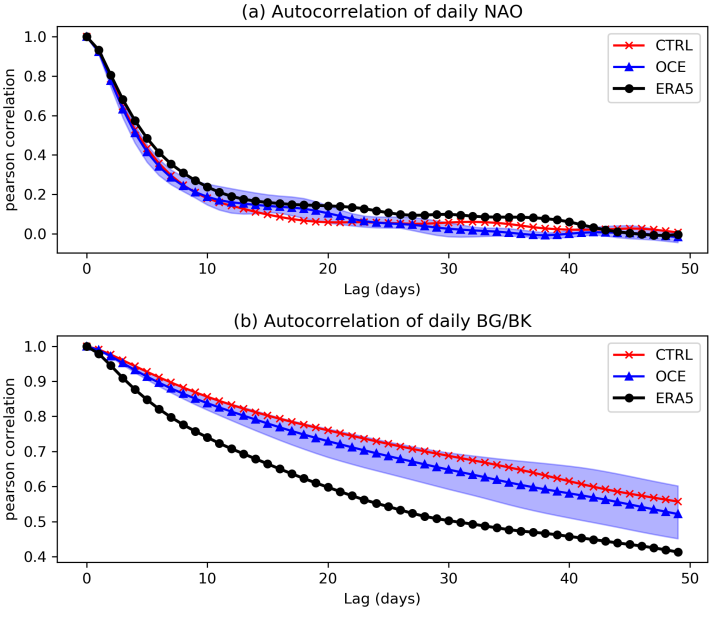


**Figure B5.** Autocorrelation of (a) the daily NAO and (b) the daily BK (resp. BG) sea ice for ERA5, black dotted (resp. CTRL, red crosses, and OCE, blue triangles). Data is restricted to days in November through February, 1980-2015. Shading indicates the ensemble spread of OCE: the CTRL spread (not shown) is similar in extent.

https://doi.org/10.5194/wcd-2021-61
Preprint. Discussion started: 1 October 2021


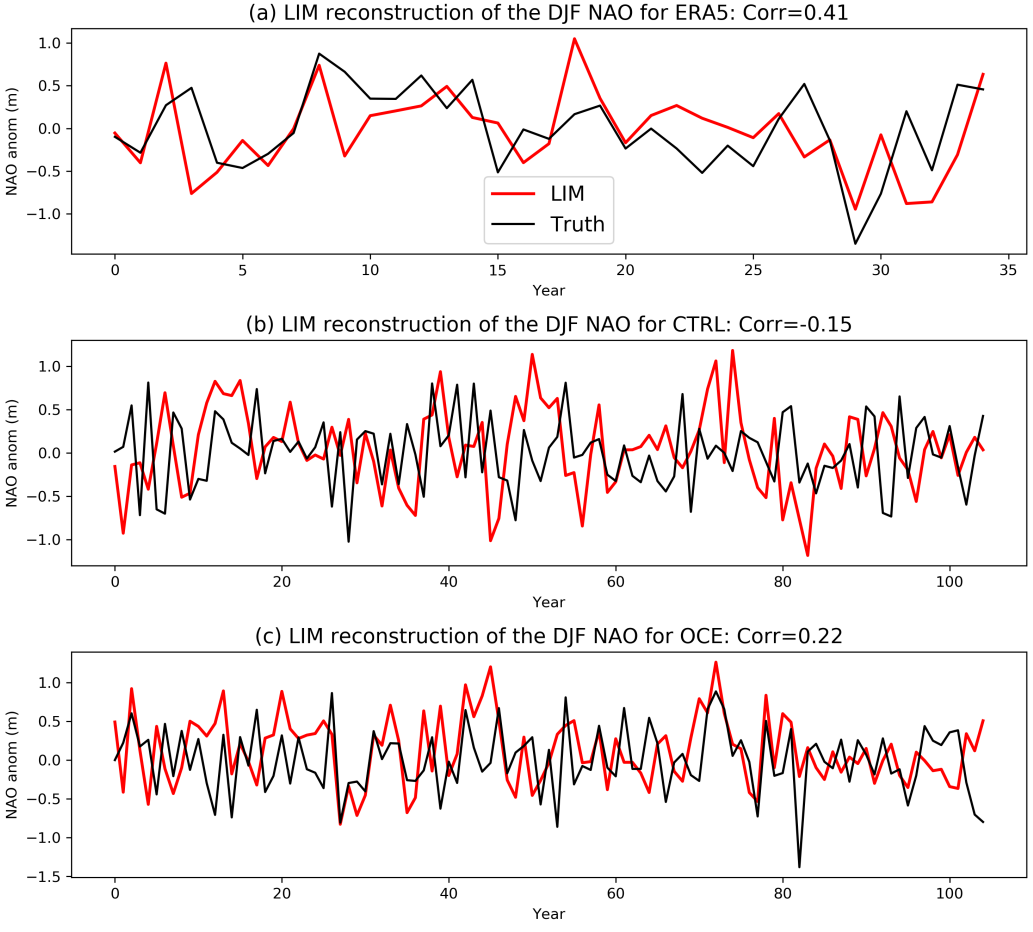


**Figure B6.** Predictions of the DJF NAO timeseries using the LIM initialised each 1st of November. For (a) ERA5, (b) CTRL and (c) OCE. Each individual data set covers the 35 years 1980-2015, but the ensemble members of CTRL and OCE have been concatenated together, and therefore cover 105 years. In each plot, the LIM prediction is in red and the true timeseries in black. The value Corr in each title is the Pearson correlation between the two timeseries.

https://doi.org/10.5194/wcd-2021-61
Preprint. Discussion started: 1 October 2021


*Author contributions.* KS and SJ jointly generated the main model simulations used. KS performed the analysis, created the plots and led the writing of the manuscript. SJ developed and implemented the stochastic schemes used and assisted in the writing of the manuscript and interpretation of results.

*Competing interests.* We declare there are no competing interests.

*Acknowledgements.* KS gratefully acknowledges funding from the Thomas Philips and Jocelyn Keene Junior Research Fellowship, Jesus College, Oxford. The experiments considered in this study were created as part of, and while supported by, the Horizon 2020 project PRIMAVERA (grant number 641727), funded by the European Research Council. SJ is contributing with this work to the projects M3 and L4 of the Collaborative Research Centre TRR 181 "Energy Transfer in Atmosphere and Ocean" funded by the Deutsche Forschungsgemeinschaft (DFG, German Research Foundation) under project number 274762653. The main experiments used in this study were generated using supercomputing units from an ECMWF Special Project: we thank ECMWF support staff for their patience and invaluable assistance. Conversations between KS and Fenwick Cooper were instrumental in the creation of this manuscript. In particular, the LIM analysis of our paper was heavily inspired by unpublished work of Cooper, who showed KS that a LIM can account for the teleconnection in observational data.

https://doi.org/10.5194/wcd-2021-61
Preprint. Discussion started: 1 October 2021


Weather and Climate Dynamics Discussions
Open Access
EGU

## References

Alexander, M. A., Matrosova, L., Penland, C., Scott, J. D., and Chang, P.: Forecasting Pacific SSTs: Linear inverse model predictions of the PDO, Journal of Climate, 21, 385–402, 2008.

Baker, L. H., Shaffrey, L. C., Sutton, R. T., Weisheimer, A., and Scaife, A. A.: An Intercomparison of Skill and Overconfidence/Underconfidence of the Wintertime North Atlantic Oscillation in Multimodel Seasonal Forecasts, Geophysical Research Letters, https://doi.org/10.1029/2018GL078838, 2018.

Balsamo, G., Beljaars, A., Scipal, K., Viterbo, P., van den Hurk, B., Hirschi, M., and Betts, A. K.: A Revised Hydrology for the ECMWF Model: Verification from Field Site to Terrestrial Water Storage and Impact in the Integrated Forecast System, Journal of Hydrometeorology, 10, 623–643, https://doi.org/10.1175/2008JHM1068.1, 2009.

Barnes, E. A. and Screen, J. A.: The impact of Arctic warming on the midlatitude jet-stream: Can it? Has it? Will it?, Wiley Interdisciplinary Reviews: Climate Change, https://doi.org/10.1002/wcc.337, 2015.

Berner, J., Achatz, U., Batté, L., Bengtsson, L., De La Cámara, A., Weisheimer, A., Weniger, M., Williams, P. D., and Yano, J.-I.: Stochastic parameterizations: Toward a New View of Weather and Climate Models, Bulletin of the American Meteorological Society, 98, 565–588, https://doi.org/10.1175/BAMS-D-15-00268.1, 2017.

Blackport, R. and Screen, J. A.: Observed statistical connections overestimate the causal effects of arctic sea ice changes on midlatitude winter climate, Journal of Climate, https://doi.org/10.1175/JCLI-D-20-0293.1, 2021.

Blackport, R., Screen, J. A., van der Wiel, K., and Bintanja, R.: Minimal influence of reduced Arctic sea ice on coincident cold winters in mid-latitudes, Nature Climate Change, https://doi.org/10.1038/s41558-019-0551-4, 2019.

Brankart, J.-M., Candille, G., Garnier, F., Calone, C., Melet, A., Bouttier, P.-A., Brasseur, P., and Verron, J.: A generic approach to explicit simulation of uncertainty in the NEMO ocean model, Geoscientific Model Development, 8, 1285–1297, https://doi.org/10.5194/gmd-8-1285-2015, 2015.

Christensen, H. M., Berner, J., Coleman, D. R., and Palmer, T. N.: Stochastic parameterization and El Niño-southern oscillation, Journal of Climate, 30, 17–38, https://doi.org/10.1175/JCLI-D-16-0122.1, 2017.

Davini, P., Von Hardenberg, J., Corti, S., Christensen, H. M., Juricke, S., Subramanian, A., Watson, P. A., Weisheimer, A., and Palmer, T. N.: Climate SPHINX: Evaluating the impact of resolution and stochastic physics parameterisations in the EC-Earth global climate model, Geoscientific Model Development, 10, 1383–1402, https://doi.org/10.5194/gmd-10-1383-2017, 2017.

Dawson, A. and Palmer, T. N.: Simulating weather regimes: impact of model resolution and stochastic parameterization, Climate Dynamics, 44, 2177–2193, https://doi.org/10.1007/s00382-014-2238-x, 2015.

Deser, C., Walsh, J. E., and Timlin, M. S.: Arctic sea ice variability in the context of recent atmospheric circulation trends, Journal of Climate, https://doi.org/10.1175/1520-0442(2000)013<0617:ASIVIT>2.0.CO;2, 2000.

Deser, C., Tomas, R. A., and Peng, S.: The transient atmospheric circulation response to North Atlantic SST and sea ice anomalies, Journal of Climate, https://doi.org/10.1175/JCLI4278.1, 2007.

Dunstone, N., Smith, D., Scaife, A., Hermanson, L., Eade, R., Robinson, N., Andrews, M., and Knight, J.: Skilful predictions of the winter North Atlantic Oscillation one year ahead, Nature Geoscience, 9, 809–814, https://doi.org/10.1038/ngeo2824, 2016.

Eade, R., Smith, D., Scaife, A., Wallace, E., Dunstone, N., Hermanson, L., and Robinson, N.: Do seasonal-to-decadal climate predictions underestimate the predictability of the real world?, Geophysical Research Letters, 41, 5620–5628, https://doi.org/10.1002/2014GL061146, 2014.

https://doi.org/10.5194/wcd-2021-61
Preprint. Discussion started: 1 October 2021


Frankignoul, C., Czaja, A., and L'Heveder, B.: Air-sea feedback in the North Atlantic and surface boundary conditions for ocean models, Journal of Climate, https://doi.org/10.1175/1520-0442(1998)011<2310:ASFITN>2.0.CO;2, 1998.

García-Serrano, J., Frankignoul, C., Gastineau, G., and de la Cámara, A.: On the predictability of the winter Euro-Atlantic climate: Lagged influence of autumn Arctic sea ice, Journal of Climate, https://doi.org/10.1175/JCLI-D-14-00472.1, 2015.

Gent, P. R. and Mcwilliams, J. C.: Isopycnal Mixing in Ocean Circulation Models, Journal of Physical Oceanography, 20, 150 – 155, https://doi.org/10.1175/1520-0485(1990)020<0150:IMIOCM>2.0.CO;2, 1990.

Haarsma, R., Acosta, M., Bakhshi, R., Bretonnière, P.-A., Caron, L.-P., Castrillo, M., Corti, S., Davini, P., Exarchou, E., Fabiano, F., Fladrich, U., Fuentes Franco, R., García-Serrano, J., von Hardenberg, J., Koenigk, T., Levine, X., Meccia, V. L., van Noije, T., van den Oord, G., Palmeiro, F. M., Rodrigo, M., Ruprich-Robert, Y., Le Sager, P., Tourigny, E., Wang, S., van Weele, M., and Wyser, K.: HighResMIP versions of EC-Earth: EC-Earth3P and EC-Earth3P-HR – description, model computational performance and basic validation, Geoscientific Model Development, 13, 3507–3527, https://doi.org/10.5194/gmd-13-3507-2020, 2020.

Hawkins, E. and Sutton, R.: Decadal predictability of the Atlantic Ocean in a coupled GCM: Forecast skill and optimal perturbations using linear inverse modeling, Journal of Climate, 22, 3960–3978, 2009.

Hersbach, H., Bell, B., Berrisford, P., Hirahara, S., Horányi, A., Muñoz-Sabater, J., Nicolas, J., Peubey, C., Radu, R., Schepers, D., Simmons, A., Soci, C., Abdalla, S., Abellan, X., Balsamo, G., Bechtold, P., Biavati, G., Bidlot, J., Bonavita, M., De Chiara, G., Dahlgren, P., Dee, D., Diamantakis, M., Dragani, R., Flemming, J., Forbes, R., Fuentes, M., Geer, A., Haimberger, L., Healy, S., Hogan, R. J., Hólm, E., Janisková, M., Keeley, S., Laloyaux, P., Lopez, P., Lupu, C., Radnoti, G., de Rosnay, P., Rozum, I., Vamborg, F., Villaume, S., and Thépaut, J.-N.: The ERA5 global reanalysis, Quarterly Journal of the Royal Meteorological Society, 146, 1999–2049, https://doi.org/https://doi.org/10.1002/qj.3803, 2020.

Hoskins, B. J. and Karoly, D. J.: The steady linear response of a spherical atmosphere to thermal and orographic forcing., Journal of the Atmospheric Sciences, https://doi.org/10.1175/1520-0469(1981)038<1179:TSLROA>2.0.CO;2, 1981.

Hurrell, J. W., Kushnir, Y., Otterson, G., and Visbeck, M.: An Overview of the North Atlantic Oscillation, The North Atlantic Oscillation: Climatic Significance and Environmental Impact, 134, 263, https://doi.org/10.1029/GM134, 2003.

Juricke, S. and Jung, T.: Influence of stochastic sea ice parametrization on climate and the role of atmosphere-sea ice-ocean interaction, Philosophical Transactions of the Royal Society A: Mathematical, Physical and Engineering Sciences, 372, https://doi.org/10.1098/rsta.2013.0283, 2014.

Juricke, S., Lemke, P., Timmermann, R., and Rackow, T.: Effects of Stochastic Ice Strength Perturbation on Arctic Finite Element Sea Ice Modeling, Journal of Climate, 26, 3785 – 3802, https://doi.org/10.1175/JCLI-D-12-00388.1, 2013.

Juricke, S., Goessling, H. F., and Jung, T.: Potential sea ice predictability and the role of stochastic sea ice strength perturbations, Geophysical Research Letters, 41, 8396–8403, https://doi.org/https://doi.org/10.1002/2014GL062081, 2014.

Juricke, S., Palmer, T. N., and Zanna, L.: Stochastic sub-grid scale ocean mixing: Impacts on low frequency variability, Journal of Climate, pp. JCLI–D–16–0539.1, https://doi.org/10.1175/JCLI-D-16-0539.1, 2017.

Juricke, S., MacLeod, D., Weisheimer, A., Zanna, L., and Palmer, T. N.: Seasonal to annual ocean forecasting skill and the role of model and observational uncertainty, Quarterly Journal of the Royal Meteorological Society, 144, 1947–1964, https://doi.org/https://doi.org/10.1002/qj.3394, 2018.

Keeley, S. P., Sutton, R. T., and Shaffrey, L. C.: The impact of North Atlantic sea surface temperature errors on the simulation of North Atlantic European region climate, Quarterly Journal of the Royal Meteorological Society, https://doi.org/10.1002/qj.1912, 2012.

https://doi.org/10.5194/wcd-2021-61
Preprint. Discussion started: 1 October 2021


Kim, B. M., Son, S. W., Min, S. K., Jeong, J. H., Kim, S. J., Zhang, X., Shim, T., and Yoon, J. H.: Weakening of the stratospheric polar vortex by Arctic sea-ice loss, Nature Communications, https://doi.org/10.1038/ncomms5646, 2014.

Koenigk, T. and Brodeau, L.: Arctic climate and its interaction with lower latitudes under different levels of anthropogenic warming in a global coupled climate model, Climate Dynamics, https://doi.org/10.1007/s00382-016-3354-6, 2017.

Koenigk, T., Mikolajewicz, U., Jungclaus, J. H., and Kroll, A.: Sea ice in the Barents Sea: Seasonal to interannual variability and climate feedbacks in a global coupled model, Climate Dynamics, https://doi.org/10.1007/s00382-008-0450-2, 2009.

Koenigk, T., Caian, M., Nikulin, G., and Schimanke, S.: Regional Arctic sea ice variations as predictor for winter climate conditions, Climate Dynamics, https://doi.org/10.1007/s00382-015-2586-1, 2016.

Kretschmer, M., Coumou, D., Donges, J. F., and Runge, J.: Using causal effect networks to analyze different arctic drivers of midlatitude winter circulation, Journal of Climate, https://doi.org/10.1175/JCLI-D-15-0654.1, 2016.

Lavergne, T., Sørensen, A. M., Kern, S., Tonboe, R., Notz, D., Aaboe, S., Bell, L., Dybkjær, G., Eastwood, S., Gabarro, C., Heygster, G., Killie, M. A., Brandt Kreiner, M., Lavelle, J., Saldo, R., Sandven, S., and Pedersen, L. T.: Version 2 of the EUMETSAT OSI SAF and ESA CCI sea-ice concentration climate data records, The Cryosphere, 13, 49–78, https://doi.org/10.5194/tc-13-49-2019, 2019.

Madec, G. and the NEMO team: NEMO ocean engine version 3.6 stable, Note du Pôle de modélisation de l'Institut Pierre-Simon Laplace, 27, 2016.

Newman, M., Sardeshmukh, P. D., and Penland, C.: How important is air-sea coupling in ENSO and MJO evolution?, Journal of Climate, https://doi.org/10.1175/2008JCLI2659.1, 2009.

Notz, D. and Community, S.: Arctic Sea Ice in CMIP6, Geophysical Research Letters, 47, e2019GL086 749, https://doi.org/https://doi.org/10.1029/2019GL086749, e2019GL086749 10.1029/2019GL086749, 2020.

Palmer, T., Buizza, R., Jung, T., Leutbecher, M., Shutts, G. J., Steinheimer, M., and Weisheimer, A.: Stochastic Parameterization and Model Uncertainty, vol. 598, http://www.ecmwf.int/publications/, 2009.

Palmer, T. N.: Towards the probabilistic Earth-system simulator: A vision for the future of climate and weather prediction, Quarterly Journal of the Royal Meteorological Society, 138, 841–861, https://doi.org/10.1002/qj.1923, 2012.

Peings, Y. and Magnusdottir, G.: Response of the wintertime northern hemisphere atmospheric circulation to current and projected arctic sea ice decline: A numerical study with CAM5, Journal of Climate, https://doi.org/10.1175/JCLI-D-13-00272.1, 2014.

Penland, C. and Magorian, T.: Prediction of Niño 3 sea surface temperatures using linear inverse modeling, Journal of Climate, 6, 1067–1076, 1993.

Penland, C. and Sardeshmukh, P.: The optimal growth of tropical sea surface temperature anomalies, J. Climate, 8, 1999–2024, 1995.

Sanchez, C., Williams, K. D., and Collins, M.: Improved stochastic physics schemes for global weather and climate models, Quart. J. Roy. Meteor. Soc., 2015.

Scaife, A. A. and Smith, D.: A signal-to-noise paradox in climate science, npj Climate and Atmospheric Science, https://doi.org/10.1038/s41612-018-0038-4, 2018.

Screen, J. A., Deser, C., Smith, D. M., Zhang, X., Blackport, R., Kushner, P. J., Oudar, T., McCusker, K. E., and Sun, L.: Consistency and discrepancy in the atmospheric response to Arctic sea-ice loss across climate models, Nature Geoscience, https://doi.org/10.1038/s41561-018-0059-y, 2018.

Siegert, S., Stephenson, D. B., Sansom, P. G., Scaife, A. A., Eade, R., and Arribas, A.: A Bayesian framework for verification and recalibration of ensemble forecasts: How uncertain is NAO predictability?, Journal of Climate, 29, 995–1012, https://doi.org/10.1175/JCLI-D-15-0196.1, 2016.

https://doi.org/10.5194/wcd-2021-61
Preprint. Discussion started: 1 October 2021


Siew, P. Y. F., Li, C., Sobolowski, S. P., and King, M. P.: Intermittency of Arctic–mid-latitude teleconnections: stratospheric pathway between autumn sea ice and the winter North Atlantic Oscillation, Weather and Climate Dynamics, https://doi.org/10.5194/wcd-1-261-2020, 2020.

Stroeve, J. and Notz, D.: Changing state of Arctic sea ice across all seasons, https://doi.org/10.1088/1748-9326/aade56, 2018.

Strommen, K. and Palmer, T. N.: Signal and noise in regime systems: A hypothesis on the predictability of the North Atlantic Oscillation, Quarterly Journal of the Royal Meteorological Society, https://doi.org/10.1002/qj.3414, 2019.

Strømmen, K., Christensen, H. M., Berner, J., and Palmer, T. N.: The impact of stochastic parametrisations on the representation of the Asian summer monsoon, Climate Dynamics, 0, 1–14, https://doi.org/10.1007/s00382-017-3749-z, 2017.

Strommen, K., Christensen, H. M., Macleod, D., Juricke, S., and Palmer, T. N.: Progress towards a probabilistic Earth system model: Examining the impact of stochasticity in the atmosphere and land component of EC-Earth v3.2, Geoscientific Model Development, https://doi.org/10.5194/gmd-12-3099-2019, 2019.

Strong, C. and Magnusdottir, G.: The role of Rossby wave breaking in shaping the equilibrium atmospheric circulation response to North Atlantic boundary forcing, Journal of Climate, https://doi.org/10.1175/2009JCLI2676.1, 2010.

Strong, C. and Magnusdottir, G.: Dependence of NAO variability on coupling with sea ice, Climate Dynamics, https://doi.org/10.1007/s00382-010-0752-z, 2011.

Sun, L., Deser, C., and Tomas, R. A.: Mechanisms of stratospheric and tropospheric circulation response to projected Arctic sea ice loss, Journal of Climate, https://doi.org/10.1175/JCLI-D-15-0169.1, 2015.

Vancoppenolle, M., Bouillon, S., Fichefet, T., Goosse, H., Lecomte, O., Morales Maqueda, M. A., and Madec, G.: The Louvain-la-Neuve sea ice model, Note du Pôle de modélisation de l'Institut Pierre-Simon Laplace, 31, 2012.

Vidale, P. L., Hodges, K., Vannière, B., Davini, P., Roberts, M. J., Strommen, K., Weisheimer, A., Plesca, E., and Corti, S.: Impact of stochastic physics and model resolution on the simulation of tropical cyclones in climate GCMs, Journal of Climate, https://doi.org/10.1175/JCLI-D-20-0507.1, 2021.

Vinje, T.: Anomalies and trends of sea-ice extent and atmospheric circulation in the Nordic Seas during the period 1864-1998, Journal of Climate, https://doi.org/10.1175/1520-0442(2001)014<0255:AATOSI>2.0.CO;2, 2001.

Von Storch, J. S.: Signatures of air-sea interactions in a coupled atmosphere-ocean GCM, Journal of Climate, https://doi.org/10.1175/1520-0442(2000)013<3361:SOASII>2.0.CO;2, 2000.

Wang, C., Zhang, L., Lee, S.-K., Wu, L., and Mechoso, C. R.: A global perspective on CMIP5 climate model biases, Nature Climate Change, 4, 201–205, 2014.

Wang, L., Ting, M., and Kushner, P. J.: A robust empirical seasonal prediction of winter NAO and surface climate, Scientific Reports, 7, 279, https://doi.org/10.1038/s41598-017-00353-y, 2017.

Warner, J. L., Screen, J. A., and Scaife, A. A.: Links Between Barents-Kara Sea Ice and the Extratropical Atmospheric Circulation Explained by Internal Variability and Tropical Forcing, Geophysical Research Letters, https://doi.org/10.1029/2019GL085679, 2020.

Watson, P. A. G., Berner, J., Corti, S., Davini, P., von Hardenberg, J., Sanchez, C., Weisheimer, A., and Palmer, T. N.: The impact of stochastic physics on tropical rainfall variability in global climate models on daily to weekly timescales, Journal of Geophysical Research: Atmospheres, 122, 5738–5762, https://doi.org/10.1002/2016JD026386, 2017.

Woollings, T., Hannachi, A., and Hoskins, B.: Variability of the North Atlantic eddy-driven jet stream, Quarterly Journal of the Royal Meteorological Society, 136, 856–868, https://doi.org/10.1002/qj.625, 2010.